

APPROVAL SHEET

Title of Thesis: Detection and quantitation of per- and polyfluoroalkyl substances (PFAS) in Baltimore Harbor using anion-exchange membrane-based passive samplers

Name of Candidate: Margaret Therese Siao
Master of Science, 2025

Thesis and Abstract Approved: _____

Lee Blaney
Professor
Chemical Biochemical and Environmental
Engineering (CBEE)

Date Approved: _____

CURRICULUM VITAE

Name: Margaret Therese Siao

Degree and date to be conferred: M.S., 2025

Secondary education: August 2015 – Jun 2019
Baltimore Polytechnic Institute, Baltimore, MD

Collegiate institutions attended: August 2019 – May 2023
University of Maryland Baltimore County
Bachelor of Science (Chemical Engineering)

August 2023 – May 2025
University of Maryland Baltimore County
Master of Science (Chemical and Biochemical Engineering)

Major: Chemical and Biochemical Engineering

Presentations: Blaney, L.; He, K.; Bett, A.; Hamidi, D.; **Siao, M.** ER20-1073: Ion-exchange membranes as passive samplers for diverse PFAS. DOD Energy & Environment Innovation Symposium (Washington, DC), December 5, 2024.

Siao, M.; Hamidi, D.; Bett, A.; He, K.; Blaney, L. Influence of solution pH and dissolved organic matter on PFAS uptake by ion-exchange membrane-based passive samplers. Fall 2024 ACS National Meeting (Denver, CO), August 20, 2024.

Hamidi, D.; He, K.; **Siao, M.**; Bett, A.; Blaney, L. Salting out of PFAS anions: Calculation of Setschenow constants. Fall 2024 ACS National Meeting (Denver, CO), August 20, 2024.

He, K.; **Siao, M.**; Hamidi, D.; Bett, A.; Blaney, L. Evaluating salting out phenomena for PFAS interactions with ion-exchange materials. Environmental Sciences: Water Gordon Research Conference (Holderness, NH), June 26, 2024.

Lorah, M.M.; Mumford, A.; Akob, D.M.; Harris, C.; Linhoff, B.; He, K.; Blaney, L.; **Siao, M.**; Hamidi, D. Enhanced biodegradation of per- and polyfluoroalkyl substances (PFAS) in semi-arid region soils in areas of aqueous film-forming foam release. Thirteenth International Conference on Remediation of Chlorinated and Recalcitrant Compounds (Denver, CO), June 2-6, 2024.

Siao, M.; Hamidi, D.; Bett, A.; He, K.; Blaney, L. Influence of water quality on PFAS uptake by ion-exchange membrane-based passive samplers. 2024 Chesapeake Water Environment Association and Chesapeake Section of the American Water Works Association Joint Spring Meeting (Perryville, MD), May 23, 2024.

He, K.; **Siao, M.**; Liang, J.; Hamidi, D.; Bett, A.; Chen, H.; Stewart, K.; Blaney, L.; Ion-exchange membranes as passive samplers for chemically-diverse PFAS. ICARE Co-Navigator Spring 2024, (Baltimore, MD), February 23, 2024.

Bett, A.; **Siao, M.**; Hamidi, D.; He, K.; Blaney, L. Influence of solution pH on PFAS accumulation in a novel equilibrium passive sampler. UMBC Undergraduate Research and Creative Achievement Day (Baltimore, MD), April 10, 2024.

He, K.; Liang, J.; **Siao, M.**; Ellington, M.; Chen, H.; Stewart, K.; Blaney, L. Development of anion-exchange membranes as passive samplers for diverse per- and polyfluoroalkyl substances. Fall 2023 ACS National Meeting (San Francisco, CA), August 13-17, 2023.

Braithwaite, S.; He, K.; **Siao, M.**; Liang, J.; Cho, Y.; Blaney, L. Impact of pH on uptake of per- and polyfluoroalkyl substances (PFAS) by anion-exchange membranes. UMBC Summer Undergraduate Research Fest (Baltimore, MD), August 9, 2023.

Ellington, M.; He, K.; **Siao, M.**; Blaney, L. Improving transformation efficiency, recovery efficiency, and throughput for total oxidizable precursor analysis of biosolids and sediment. Spring 2023 ACS National Meeting (Indianapolis, IN), March 26-30, 2023.

Siao, M.; Ellington, M.; He, K.; Blaney, L. Reducing organic interferences for PFAS analysis in biosolids. Spring 2023 ACS National Meeting (Indianapolis, IN), March 26-30, 2023.

He, K.; Amurrio, F.; Chen, H.; Dugan, C.; Ellington, M.; Feerick, A.; **Siao, M.**; Stewart, K.; Blaney, L. PFAS interactions with ion-exchange membranes: towards development of passive samplers. SERDP & ESTCP Symposium (Arlington, VA), December 1, 2022.

Ellington, M.; He, K.; **Siao, M.**; Liang, J.; Blaney, L. Total oxidizable precursor assay for PFAS: improving transformation, recovery, and throughput for soil samples. Maryland Water

Monitoring Council (Baltimore, MD),
November 17, 2023.

Professional positions held:

Graduate Research Assistant
(August 2023 – May 2025)
University of Maryland, Baltimore County

ABSTRACT

Title of Document: DETECTION AND QUANTITATION OF
PER- AND POLYFLUOROALKYL
SUBSTANCES (PFAS) IN BALTIMORE
HARBOR USING ANION-EXCHANGE
MEMBRANE-BASED PASSIVE
SAMPLERS.

Margaret Therese Siao, M.S. of Science, 2025

Directed By: Professor Lee Blaney, Department of Chemical
Biochemical and Environmental Engineering
(CBEE)

Per- and polyfluoroalkyl substances (PFAS) are synthetic chemicals commonly used in consumer and industrial products. For over 60 years, PFAS have contaminated water supplies; however, long-term, average concentrations in most water resources remain unknown. The objective of this thesis was to develop and validate the performance of a novel passive sampling device that employs anion-exchange membranes to measure time-averaged concentrations of over 20 PFAS in water. We evaluated the impacts of pH, salinity, and dissolved organic matter content on the selective uptake of PFAS with variable physicochemical properties (*e.g.*, chain length, head group) using batch reactors. Selectivity coefficients, the key calibration

parameter for the passive samplers, were calculated by measuring PFAS and chloride concentrations in water and membrane phases. Trends between selectivity coefficients and PFAS properties were identified. Selectivity coefficients varied with pH for PFAS with sulfonamide moieties, but a speciation-based model was successfully fit to the experimental data. Dissolved organic matter served as a competing anion but did not affect measured selectivity coefficients, suggesting negligible impacts on passive sampler calibration. Samplers were field-validated at four locations in and around Baltimore Harbor. They were deployed for two, three, and four weeks, with grab samples collected at deployment and retrieval. Using the universal calibration, selectivity coefficients were derived from site-specific water quality parameters to determine PFAS concentrations in the water. The calculated PFAS concentrations demonstrated reasonable agreement with grab samples. The outcomes of this study highlight the development of passive samplers with universal calibrations for PFAS measurement in diverse water sources.

DETECTION AND QUANTITATION OF PER- AND POLYFLUOROALKYL
SUBSTANCES (PFAS) IN BALTIMORE HARBOR USING ANION-
EXCHANGE MEMBRANE-BASED PASSIVE SAMPLERS.

By

Margaret Therese Siao

Thesis submitted to the Faculty of the Graduate School of the
University of Maryland, Baltimore County, in partial fulfillment
of the requirements for the degree of
Masters of Science in
Chemical and Biochemical
Engineering
2025

© Copyright by
Margaret Therese Siao
2025

Dedication

To my family and the Blaney Lab members, my first academic family. I wouldn't be here without all of your encouragement and support.

Acknowledgements

I would like to express my sincere gratitude to my advisor and mentors, Dr. Blaney and Dr. Ke He, whose guidance, expertise, and unwavering support have been invaluable throughout this research journey. Their encouragement and mentorship challenged me to become a better researcher while cultivating a friendship I will cherish in the years to come.

I am also deeply thankful to my lab mates in the Blaney lab, especially Donya Hamidi and Alvin Bett, for their collaboration, friendship, and the many discussions that enriched my research experience. Their willingness to share ideas, troubleshoot challenges, and go along with my shenanigans has made this journey both enjoyable and rewarding.

Michelle Lorah at USGS and Barbara Johnson at Blue Water Baltimore provided the guidance and expertise that elevated the outcomes of this project. They both generously took the time to mentor and help me make this project a success despite external factors making it incredibly difficult.

I extend my appreciation to my ICARE cohort and the ICARE master's program, for fostering an intellectually stimulating environment and providing the resources necessary to pursue this work. The lessons I learned with you on DEIJ and community engagement in environmental research in those late classes will stay with me in whatever I pursue in the future.

A special thank you to my family, whose unwavering belief in me has been a constant source of strength. Thank you for being my practice audiences even when you had no idea what I was talking about.

Finally, I gratefully acknowledge the financial support from the National Science Foundation (NSF) and the Department of Defense (DoD). Their funding made this research possible and has contributed significantly to advancing knowledge in this field.

Table of Contents

Dedication	ii
Acknowledgements	iii
Table of Contents	v
List of Tables	vii
List of Figures	viii
Chapter 1: Introduction and Background.....	1
1.1. Motivation and Specific Aims	1
1.2. Prior research on PFAS monitoring with passive samplers.....	4
1.3. PFAS contamination concerns in Baltimore Harbor	8
Chapter 2: Constructing the universal calibration for PFAS in anion-exchange membrane-based passive samplers	10
2.1. Introduction.....	10
2.2. Materials and Methods.....	10
2.2.2 Anion-exchange membrane specifications	12
2.1.3. Experimental design of batch sorption studies	13
2.2.4. Aqueous sample processing.....	15
2.2.5. Membrane sample processing.....	16
2.2.6. Analytical methods	16
2.3. Results and Discussion	17
2.3.1. Impact of solution pH	18
2.3.2. Impact of salt type and concentration	21
2.3.3. Impact of pH and salt concentration on the sulfonamide/o PFAS.....	24
2.3.4 Impact of DOM type and content	27
2.4. Conclusions.....	30
Chapter 3: Passive sampler field deployments to measure PFAS concentrations in and around Baltimore Harbor	32
3.1. Introduction.....	32
3.2. Materials and Methods.....	33
3.2.1. Chemical reagents	33

3.2.3 Field sampling campaign	35
3.2.4 PFAS analysis in grab samples from Baltimore Harbor	36
3.2.5. Passive sampler deployment and processing	38
3.2.6. Analytical methods	41
3.3. Results and Discussion	43
3.3.1. PFAS concentrations in grab samples from initial field campaign.....	43
3.3.2. Optimization of passive sampler design	44
3.3.3. Evaluation of required deployment time.....	46
3.3.4. Back-calculations of time-averaged PFAS levels at field sites	47
3.4. Conclusions.....	51
Chapter 4: Conclusion.....	53
Overall conclusions.....	53
4.1. Water quality impacts on PFAS selectivity coefficients for the development of a universal calibration.....	53
4.2. Passive sampler field-validations utilizing the constructed universal calibration	54
4.3. Raising awareness of PFAS contamination in the harbor through the dissemination of information to collaborators	55
4.4. Future work.....	56
Appendices.....	57
Appendix A: Abbreviation Glossary	57
Bibliography	59

List of Tables

Table 2.1. Physicochemical properties of the FAD-PET-75 anion-exchange membranes.	12
Table 2.2. Batch sorption experimental design overview.....	13
Table 2.3. Summary of the calculated "true" pK_a values and Setschenow constants for protonated and deprotonated PFAS used in Eq. 2.7.	26
Table 2.1 Physicochemical properties of the FAD-PET-75 anion-exchange membranes.	34
Table 3.1. The water quality conditions at each sampling location.....	49

List of Figures

Figure 1.1 Graphical representation of specific aims and expected outcomes to report for the project.	3
Figure 2.1. Selectivity coefficients for PFAS ⁻ over Cl ⁻ plotted as a function of (a) head group and chain length and (b) solution pH.....	19
Figure 2.2. Selectivity coefficients for (a) PFOSA, (b) N-MeFOSAA, and (c) N-EtFOSAA over Cl ⁻ at pH 2–12.....	21
Figure 2.3. Selectivity coefficients for PFAS ⁻ over Cl ⁻ measured in the presence of variable NaCl.	22
Figure 2.4. Solving for Setschenow constants: (a) calculated vs. measured selectivity coefficients for PFAS ⁻ over Cl ⁻ ; (b) calculated Setschenow constants for PFAS of concern; and (c) apparent selectivity coefficients for perfluoroalkane sulfonates (as representatives) as a function of NaCl concentration.	23
Figure 2.5. The (a) measured selectivity coefficients and (b) calculated Setschenow constants for PFCAs, PFSA, and FTSS.	24
Figure 2.6. Apparent selectivity coefficients for (a) PFOSA, (b) N-MeFOSAA, and (c) N-EtFOSAA over Cl ⁻ as a function of solution pH and salt concentration..	26
Figure 2.7. Selectivity coefficients for (a) PFOSA, (b) N-MeFOSAA, and (c) N-EtFOSAA over Cl ⁻ calculated from Eq. 2.7 plotted against experimentally measured values.	27
Figure 2.8. Measured selectivity coefficients for PFAS ⁻ over Cl ⁻ in solutions containing 1 and 10 mg L ⁻¹ (a) DOM, (b) FA, and (c) HA plotted against those for solutions with no DOM, FA, or HA.	28
Figure 2.9. Membrane-phase PFAS concentrations for solutions with 1 and 10 mg L ⁻¹ (a) DOM, (b) FA, and (c) HA.	29
Figure 2.1 Passive sampler devices were constructed with protective (a) stainless-steel and (b) copper mesh and deployed in and around Baltimore Harbor.....	35
Figure 3.1 Passive sampler devices were constructed with protective (a) stainless-steel and (b) copper mesh and deployed in and around Baltimore Harbor.	35
Figure 3.2. Map of sampling sites in and around Baltimore Harbor.	36

Figure 3.3. Sample deployment and retrieval.	39
Figure 3.4. Passive sampler retrieval and processing.	41
Figure 3.5. Total PFAS concentrations detected in preliminary grab samples.....	44
Figure 3.6. Comparison of PFAS mass accumulated in passive samplers with stainless-steel and copper protective mesh during (a) two- and (b) three-week deployments.	46
Figure 3.7. Comparison of PFAS mass accumulated on the membrane for (a) two- and three-week deployments and (b) three- and four-week deployments.	46
Figure 3.8. Mass and composition of PFAS accumulated on the passive samplers deployed at (a) Mr. Trash Wheel, (b) Prof. Trash Wheel, (c) Gwynnda Trash Wheel, and (d) wastewater effluent.....	48
Figure 3.9. PFAS concentrations determined from passive samplers plotted against those measured in grab samples.....	51

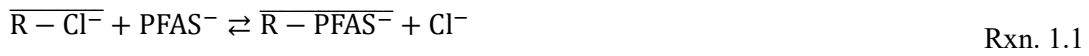
Chapter 1: Introduction and Background

1.1. Motivation and Specific Aims

Per- and polyfluoroalkyl substances (PFAS) are a group of synthetic chemicals invented in the mid-1900s for use in nonstick, waterproof, and stainproof consumer products [1], [2]. The development and use of PFAS increased when they were incorporated into aqueous film-forming foams to train for and combat jet fuel fires at military bases, airports, and other locations [3]. Due to the strong carbon-fluorine bonds, PFAS are resistant to degradation in the natural environment and engineered water/wastewater treatment processes, leading to PFAS being coined "forever chemicals" [4], [5], [6]. Given their widespread use and persistent nature, PFAS have been detected in air, soil, wastewater, surface water, groundwater, and drinking water [7], [8], [9]. Low concentrations of PFAS cause adverse human health effects, including liver damage, disruption of reproductive and immune systems, and cancer [6,7]. The Environmental Protection Agency (EPA) recently established new maximum contaminant levels for five individual PFAS in drinking water: 4 ng L⁻¹ PFOA; 4 ng L⁻¹ PFOS; 10 ng L⁻¹ PFHxS; 10 ng L⁻¹ PFNA; and 10 ng L⁻¹ HFPO-DA [2], [12]. Note, the full names of each PFAS referenced are provided in Appendix A: Abbreviation Glossary. These levels are among the lowest published regulations for any chemical contaminants.

PFAS monitoring has typically been conducted through grab sampling, which involves collecting discrete samples into bottles at specific locations and times. While helpful, the collection of grab samples is time- and labor-intensive and only informs

contaminant concentrations at certain times. Passive sampling is an alternative approach, wherein devices are placed in the environment for an extended time, accumulate contaminants, and are then collected and analyzed to back-calculate the average contaminant concentration during the deployment period [13]. Previous studies have used polyethylene-based samplers to measure conventional, hydrophobic pollutants like polychlorinated biphenyls [14]. Due to their hydrophilic head groups, PFAS require a different approach. Recent studies have shown that anion-exchange resins exhibit high selectivity for PFAS during drinking water treatment [10-12]. The reaction between PFAS and anion-exchange membranes is given by Rxn. 1.1. The relative affinity of the passive sampler for PFAS over a background ion is defined as the selectivity coefficient ($K_{Cl^-}^{PFAS^-}$; Eq. 1.1), which was calculated using the $[PFAS^-]$ and $[Cl^-]$ measured in the aqueous and membrane phase..



$$K_{Cl^-}^{PFAS^-} = \frac{[PFAS^-]_{mem}[Cl^-]_{aq}}{[Cl^-]_{mem}[PFAS^-]_{aq}} \quad \text{Eq. 1.1}$$

The objective of this project was to develop, calibrate, and validate novel passive samplers that employ anion-exchange membranes to quantify time-averaged concentrations for over 20 PFAS at levels as low as 1 ng L⁻¹. I hypothesize that samplers equipped with anion-exchange membranes will accumulate PFAS according to Rxn. 1.1, enabling PFAS quantitation via Eq. 1.1. The proposed passive sampler needs to be (i) calibrated for variable water quality conditions and (ii) validated in

real waters to confirm the accuracy, precision, and sensitivity of PFAS analysis.

Aim 1: Determine the impacts of solution pH, salinity, and dissolved organic matter (DOM) content on the uptake and selectivity for 22 PFAS with variable physicochemical properties (*e.g.*, chain length, head group) by the anion-exchange membrane and develop a universal calibration for the passive samplers.

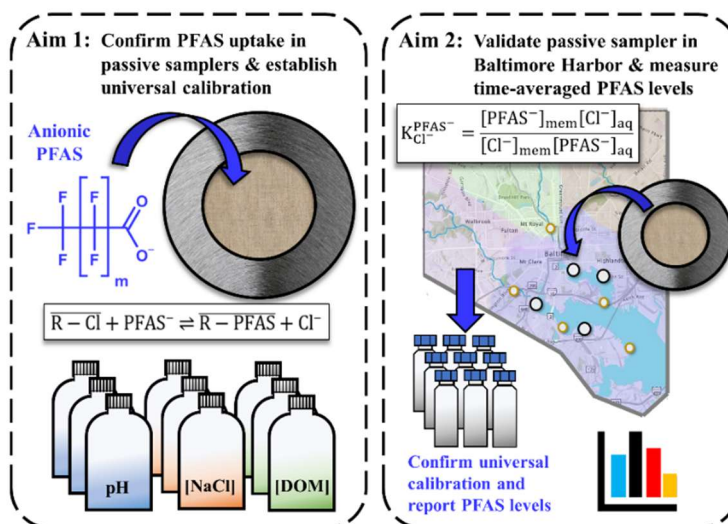


Figure 1.1. Graphical representation of specific aims and expected outcomes to report for the project. The universal calibration constructed in Aim 1 will be validated by

conducting field deployments in and around the Baltimore Harbor (Aim 2) to assess the extent of contamination and provide relevant information to surrounding local communities.

1.2. Prior research on PFAS monitoring with passive samplers

The increasing interest in PFAS has led to extensive research on various aspects of their occurrence, fate, and transport in the environment. PFAS analysis is key to these studies. In recent years, sampling methodologies have shifted from traditional grab sampling to passive sampling due to its practical advantages related to time and resource management [13]. However, a significant challenge associated with passive sampling is the need for rigorous calibration to ensure the accuracy and reliability of calculated concentrations. Passive samplers often require extensive and complex calibration to provide precise and representative measurements in different water sources. The performance of many passive samplers is influenced by environmental factors (*e.g.*, flow rate, pH, salinity, DOM, temperature) that affect the extent and/or rate of PFAS uptake [17], [18]. Therefore, thorough calibration and validation under variable field conditions are essential to ensure the reliability of passive sampling approaches to PFAS monitoring. Tailored calibrations for a specific site limit the utility of passive samplers, increase the potential for inaccurate back-calculations, affect the ease of deployments, and require additional time. As a result, new passive sampling strategies that involve universal calibration are needed.

Equilibrium and kinetic (integrative) samplers are the two primary categories of passive samplers used to monitor environmental contaminants. Equilibrium passive samplers function by accumulating contaminants until thermodynamic equilibrium is reached between the sampler and the surrounding environment (*e.g.*, water, air,

sediment). The key calibration parameter is the equilibrium constant for the partitioning reaction, which is typically determined by the contaminant concentration in the sampler and water as a partition constant (K_d) [19], [20]. For conventional equilibrium samplers, water quality affects the K_d value, mandating calibration in each water source for accurate results. Integrative samplers, on the other hand, accumulate contaminants according to a specific sampling rate (R_s), which is the key calibration parameter. These samplers do not reach equilibrium during deployment but rather rely on a constant R_s to estimate time-averaged concentrations over the exposure period [17], [19], [21], [22]. PFAS uptake by the sampler depends on various factors, including the target analytes and environmental conditions, such as flow velocity and temperature [23]. These environmental conditions can potentially fluctuate greatly during deployment, making the accurate determination of R_s difficult.

Multiple studies have demonstrated passive sampling for PFAS using both equilibrium and integrative samplers in both surface water and sediment pore water. A study by Medon *et.al.* used a cylindrical HDPE equilibrium sampler containing a receiving solution (*e.g.*, MilliQ water), with a polycarbonate membrane filter covering the opening, to measure PFAS in laboratory studies and field deployments. Laboratory experiments focused on PFAS sorption onto the sampler's materials, as well as bench-scale deployments to determine the PFAS mass transfer coefficient across the rate-limiting barrier. Sampler performance was evaluated through deployments at four locations around Lake Niapenco (Hamilton, Ontario), specifically near the water-sediment and air-water interfaces. [24]. Medon *et.al.*

obtained PFAS concentrations within a factor of two of concentrations measured in corresponding grab samples by accounting for temperature fluctuations and biofouling according to performance reference compound (PRC) loss rates. PRCs are isotopically-labeled compounds added to samplers prior to deployment to determine the extent of equilibrium. By tracking the depletion of PRCs over time, Medon *et.al.* could estimate the mass transfer coefficients for the target PFAS analytes. For deployments where full equilibrium was not reached, the remaining PRC concentrations were used to estimate the PFAS concentrations at equilibrium. This method involved calculating the fraction of PRC remaining in the sampler and using it to adjust the measured PFAS concentrations, thereby providing an estimate of the actual environmental concentrations [25], [26]. The effectiveness of PRCs depends on a number of factors, including regular calibration and validation, which can be labor-intensive and time-consuming. Other limitations range from cost and availability to degradation and compatibility issues [27].

A study conducted by the Norwegian Geotechnical Institute employed a polar organic chemical integrative sampler (POCIS) to monitor PFAS emissions from the paper industry and found that environmental conditions significantly influenced R_s [28]. Under static laboratory conditions, a calibration for R_s was constructed, but the authors found that the following environmental parameters affected the calibration: temperature increased R_s due to changes in PFAS diffusion across the membrane; higher flow rates increased R_s by enhancing mass transfer across the membrane; lower solution pH increased R_s due to changes in PFAS speciation and membrane interactions; but DOM content exerted minimal impacts on PFAS uptake [28], [29],

[30]. Although these effects were observed, no models or corrections were proposed to account for changes in water quality in the field. Field deployments were conducted with the laboratory-derived R_s calibration, but the actual field conditions were not fully represented by the calibration.

Many studies on POCIS sampling rates indicate that environmental factors (*e.g.*, flow rate, temperature, pH, DOM) impact R_s . However, these factors are rarely corrected for in-field calibrations [30], [31], [32]. In general, past work has shown that increased temperature, faster flow rates, and lower pH tend to enhance R_s ; the corresponding impacts of equilibrium samplers are equally complex. DOM exerted a minimal impact on R_s and did not require corrections for integrative samplers [33], [34], but the effects of DOM on equilibrium samplers are widely reported [30], [35], [36]. Although these effects are well recognized, calibrations often rely on laboratory-derived R_s or K_d values without adjustments for actual field conditions. Rather than developing mathematical models, researchers typically use empirical adjustments (*e.g.*, PRCs) and *in situ* calibrations to account for site-specific variations [27], [37].

To overcome the challenges with applying conventional equilibrium and integrative samplers for PFAS monitoring, the passive sampler reported in this thesis operates on an equilibrium-based framework designed to enable universal calibration for application in any water body. Notably, no previous studies have utilized ion-exchange membranes with selectivity coefficients as passive samplers for PFAS detection.

1.3. PFAS contamination concerns in Baltimore Harbor

Baltimore Harbor, situated at the heart of Maryland's largest city, has been a cornerstone of economic and cultural development for centuries. Since its early days as a colonial trading post, the harbor has evolved into a thriving hub of commerce and industry. Its strategic location on the Patapsco River, with access to the Chesapeake Bay and the Atlantic Ocean, made it an ideal site for the export of tobacco, grain, and other agricultural products [38], [39], [40]. As the city grew, so did the harbor's importance, becoming a major entry point for immigrants and a center for shipbuilding, steel production, and manufacturing.

Today, Baltimore Harbor is a vibrant blend of history and modernity. While the Harbor continues to serve as a significant economic center, the location has also transformed into a popular destination for tourism and recreation. The Inner Harbor, once a bustling industrial area, is now a thriving waterfront district filled with shops, restaurants, and cultural attractions [38]. However, the Harbor has faced many environmental challenges, including pollution from industrial activities and unintended sewage inputs [41]. As Baltimore continues to evolve to be accessible for everyone, the urge to improve water quality and address contaminants of emerging concern, such as PFAS, grows [41], [42], [43].

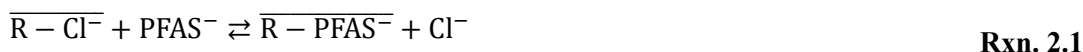
Regional research on PFAS contamination has primarily focused on drinking water treatment plants and military installations. However, organizations such as the U.S. Geological Survey (USGS), Chesapeake Bay Program, Maryland Department of the Environment (MDE), and Department of Defense (DoD) have recently expanded

investigations to assess PFAS contamination more broadly within the Chesapeake Bay watershed [44], [45], [46], [47]. Current studies are focused on PFAS bioaccumulation in local fish species present in the Harbor [48], but further research is needed to comprehensively understand the extent of PFAS contamination in the Chesapeake Bay ecosystem and the potential ecological and human health implications. The goal of this project is to employ our passive samplers to investigate PFAS contamination in key locations of Baltimore Harbor and surrounding areas to provide Maryland agencies and residents with more accurate and relevant information regarding water quality.

Chapter 2: Constructing the universal calibration for PFAS in anion-exchange membrane-based passive samplers

2.1. Introduction

Due to the pervasiveness of trace concentrations of per- and polyfluoroalkyl substances (PFAS) in the environment, reliable sampling methods are urgently needed to inform the occurrence and long-term levels of PFAS in water sources. This chapter aims to establish a universal calibration for anion-exchange membrane-based passive samplers. To achieve this goal, fundamental expressions were incorporated into Eq. 2.1 to quantify the effects of key water quality parameters, such as solution pH, salinity, and dissolved organic matter, on the selectivity coefficient for PFAS in diverse water sources. These studies were conducted through a series of controlled bench-scale experiments conducted between Spring 2023 and Spring 2024.



$$K_{\text{Cl}^-}^{\text{PFAS}^-} = \frac{[\text{PFAS}^-]_{\text{mem}}[\text{Cl}^-]_{\text{aq}}}{[\text{Cl}^-]_{\text{mem}}[\text{PFAS}^-]_{\text{aq}}} \quad \text{Eq. 2.1}$$

2.2. Materials and Methods

2.2.1 Chemical reagents

PFAS certified standards, surrogates, and internal standards were obtained from Wellington Laboratories (Ontario, Canada). Bulk PFAS options were purchased from Fisher, Sigma, or Caymanchem, and the actual concentrations were determined with the certified standards. In total, 22 bulk PFAS, including 11 perfluorocarboxylic

acids (*i.e.*, H-PFBA, H-PFPeA, H-PFHxA, H-PFHpA, H-PFOA, H-PFNA, H-PFDA, H-PFUdA, H-PFDoA, H-PFTrDA, H-PFTeDA), five perfluorosulfonate salts or perfluorosulfonic acids (*i.e.*, K-PFBS, Na-PFPeS, H-PFHxS, Na-PFHpS, Na-PFOS), three fluorotelomer sulfonate salts (*i.e.*, Na-4:2 FTS, Na-6:2 FTS, Na-8:2 FTS), and three perfluoroalkane sulfonamide or sulfonamido acetic acids (*i.e.*, H-PFOSA, H-N-MeFOSAA, H-N-EtFOSAA) were employed in laboratory experiments. 28 certified PFAS standards, along with nine mass-labeled surrogates (*i.e.*, H-M3PFBA, H-M4PFHpA, H-M8PFOA, H-MPFNA, H-MPFDoA, Na-MPFHxS, Na-M8PFOS, H-M8FOSA-I, H-d5-NEtFOSAA), and 15 mass-labeled internal standards (*i.e.*, H-MPFBA, H-M5PFPeA, H-MPFHxA, H-MPFOA, H-MPFDA, H-MPFUdA, H-M2PFTeDA, Na-M3PFBS, Na-M3PFHxS, Na-MPFOS, Na-M2-4:2FTS, Na-M2-6:2 FTS, Na-M2-8:2FTS, H-M3HFPO-DA, H-d3-NMeFOSAA) were used for tracking the performance of the entire analytical procedure. The full names of each PFAS standard and mass-labeled surrogate/internal standard, along with salient chemical properties, are provided in Appendix A: Abbreviation Glossary.

Other chemical reagents were procured from Fisher Scientific (Hampton, NH, USA). HPLC grade methanol (MeOH), acetonitrile, and ammonium acetate (NH₄Ac) were employed during solid-phase extraction (SPE) and solvent extraction of PFAS in water and membrane samples, respectively. Small volumes of 1 M hydrochloric acid (HCl) and 1 M sodium hydroxide (NaOH) were used to set and maintain the pH of batch reactors during laboratory experiments. Salts, including sodium chloride (NaCl), potassium chloride (KCl), magnesium chloride (MgCl₂), calcium chloride (CaCl₂), sodium sulfate (Na₂SO₄), and sodium bicarbonate (NaHCO₃), were added to

experimental solutions to investigate the impacts of salting out effects on PFAS interactions with anion-exchange membranes. Suwannee River natural organic matter (NOM), fulvic acids (FA), and humic acids (HA) were purchased from the International Humic Substances Society (Denver, CO, USA) to determine whether dissolved organic matter (DOM) affected PFAS uptake or selectivity. Nitric acid (HNO₃) was applied to assist with digestion of membranes from field sampling campaigns that employed passive samplers with protective copper mesh screens. LC-MS grade water, MeOH, and NH₄Ac were used during liquid chromatography with tandem mass spectrometry (LC-MS/MS). Deionized water was generated by a Neu-Ion System (Baltimore, MD, USA) for use during laboratory experiments and field sample processing.

2.2.2 Anion-exchange membrane specifications

FAD-PET-75 anion-exchange membranes were purchased from the FuelCell Store (Bryan, TX, USA) for use as passive samplers in laboratory experiments and field campaigns. Select properties of the FAD-PET-75 membranes are reported in Table 2.1.

Table 2.1. Physicochemical properties of the FAD-PET-75 anion-exchange membranes.

Membrane	Ion-exchange capacity (IEC) (meq g ⁻¹)	Mass per area (mg cm ⁻²)	Standard thickness (μm)
FAD-PET-75	2.15 ± 0.15	7.75 ± 0.75	70 ± 10

2.1.3. Experimental design of batch sorption studies

Batch experiments were conducted to generate sorption isotherms for PFAS uptake by anion-exchange membranes. The corresponding data were used to calculate the apparent selectivity coefficients for PFAS over chloride (Cl^-) under various water quality conditions (Table 2.2.). The specific water quality parameters were selected to replicate conditions in the Chesapeake Bay. In particular, $1 \times 1 \text{ cm}^2$ FAD-PET-75 coupons were added to 100-mL solutions that contained (i) 1–1000 $\mu\text{g L}^{-1}$ of individual PFAS or (ii) mixtures of 22 PFAS at 100 $\mu\text{g L}^{-1}$ (each), along with the variable water quality conditions listed in Table 2.2. Initial samples were collected before adding the membrane coupons. The temperature for all experiments was maintained at $22 \pm 2 \text{ }^\circ\text{C}$. All experiments were performed in triplicate. High-density polyethylene (HDPE) and polypropylene (PP) bottles and pipets were used during all laboratory experiments to minimize PFAS losses to containers [49].

Table 2.2. Batch sorption experimental design overview. Three variables were studied for a mix of 22 PFAS to determine the impact on $K_{\text{Cl}^-}^{\text{PFAS}^-}$.

Variable	Solution pH	Salt type	Salt concentration (mM)	DOM concentration (mg L ⁻¹)
Control	7	NaCl	10	-
Solution pH	2 – 12	NaCl	10	-
Salt type and concentration	7	KCl, MgCl ₂ , CaCl ₂ , NaSO ₄ , NaHCO ₃	1, 10, 100	-
DOM	7	NaCl	10	1, 10
Mixed effects	3 – 10	NaCl	1, 10, 100	-

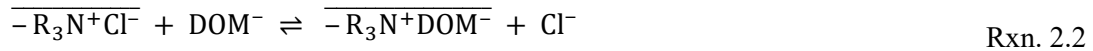
The batch reactors were shaken on an orbital mixer 250 rpm for at least five days to ensure equilibrium. Then, the membranes were removed from the reactors and

processed to quantify the membrane-phase PFAS⁻ and Cl⁻ concentrations via LC-MS/MS (section 2.2.5) and ion chromatography (section 2.2.6), respectively. Similarly, the aqueous-phase PFAS were measured from the solutions remaining in the batch reactors (sections 2.2.4 and 2.2.6). The membrane- and aqueous-phase PFAS⁻ and Cl⁻ concentrations were used to calculate the apparent selectivity coefficient ($K_{Cl^-}^{PFAS^-}|_{app}$) for the specific water quality condition using Eq. 2.1. For experiments with variable pH, salt concentration, and DOM content, the apparent selectivity coefficients were modeled using acid-base speciation (Eq. 2.2), salting out (Eq. 2.3-Eq. 2.4), and competitive adsorption (Rxn. 2.2) relationships. The fundamental parameters included in Eq. 2.2-Eq. 2.4 were used to develop an *a priori* universal calibration for passive sampler deployment in any water.

$$K_{Cl^-}^{PFAS^-}|_{app} = \left(1 + \frac{10^{-pK_a}}{10^{-pH}}\right)^{-1} K_{Cl^-}^{H-PFAS} + \left(\frac{10^{-pH}}{10^{-pK_a}} + 1\right)^{-1} K_{Cl^-}^{PFAS^-} \quad \text{Eq. 2.2}$$

$$K_{Cl^-}^{PFAS^-}|_{salt} = 10^{(+K^S[salt])} K_{Cl^-}^{PFAS^-}|_{DI} \quad \text{Eq. 2.3}$$

$$K_{Cl^-}^{PFAS^-}|_{salt} = K_{Cl^-}^{PFAS^-}|_{10^{-1} \text{ M NaCl}} 10^{(+K^S[salt] - 10^{-1} K^S)} \quad \text{Eq. 2.4}$$



In Eq. 2.2-Eq. 2.4, pK_a is the negative value of the log-transformed acid dissociation constant for the PFAS, $K_{Cl^-}^{H-PFAS}$ is the selectivity coefficient for the neutral form of PFAS, and the K^S is the Setschenow constant that quantifies the salting-out effects on PFAS in experimental solutions.

2.2.4. Aqueous sample processing

Aqueous-phase PFAS⁻ concentrations were determined by first transferring 10 mL of solution from each batch reactor into a 15-mL HDPE centrifuge tube. Then, each sample was spiked with 50 µL of a 50 µg L⁻¹ mixture of nine mass-labeled surrogates. Solid-phase extraction was conducted using 0.1% NH₄Ac in MeOH (HPLC) to condition the WAX cartridge, 50% MeOH in DI water to rinse the WAX cartridge, and 5% NH₄Ac in acetonitrile was used to elute the PFAS from the cartridge. The extracts were dried to completeness in a nitrogen evaporator and reconstituted for LC-MS/MS analysis with 50 µL of a 50 µg L⁻¹ mixture of 15 mass-labeled internal standards, 200 µL of 20 mM NH₄Ac in MeOH, and 250 µL of DI water.

The aqueous-phase Cl⁻ concentrations were determined by mass balance using the ion-exchange capacity (IEC) of the FAD-PET-75 membrane and the initial Cl⁻ concentration from the experimental design (Table 2.2) using Eq. 2.5-Eq. 2.6.

$$q_{\text{Cl}^-} = \text{IEC} - \sum q_{\text{PFAS}} \quad \text{Eq. 2.5}$$

$$[\text{Salt}]_{\text{aq}} = [\text{Salt}]_{\text{aq,initial}} + \sum q_{\text{PFAS}_m} \quad \text{Eq. 2.6}$$

In Eq. 2.5-Eq. 2.6, q_{Cl^-} is the remaining Cl⁻ concentration on the membrane (meq g⁻¹), q_{PFAS} is the PFAS⁻ concentration on the membrane (meq g⁻¹). The $[\text{Salt}]_{\text{aq,initial}}$ and $[\text{Salt}]_{\text{aq}}$ represent the initial and final aqueous salt concentrations respectively (meq L⁻¹).

2.2.5. Membrane sample processing

Once batch reactors were removed from the orbital shaker, the 1×1 cm² membrane coupons were collected, rinsed with DI water, and air-dried. The dry weight was recorded for each membrane. Then, the membranes were transferred to 15-mL HDPE centrifuge tubes for digestion with 10 mL MeOH [50]. Samples were vortexed, placed in a sonicator for 15 min at 50 °C to ensure the release of PFAS from the membrane, and centrifuged for 10 min at 5,000 rpm. Samples were then diluted 10× and 100× with 50 µL of a 50 µg L⁻¹ mixture of 15 mass-labeled internal standards, 50 µL supernatant, and 400 µL 10 mM NH₄Ac in 40% MeOH. The following two-step process was employed for the 100× dilution: (i) 50 µL supernatant + 400 µL 10 mM NH₄Ac in 40% MeOH; and (ii) 50 µL of 50 µg L⁻¹ mix 15 mass-labeled internal standards + 50 µL working solution + 400 µL 10 mM NH₄Ac in 40% MeOH.

2.2.6. Analytical methods

PFAS concentrations in reconstituted extracts from the water and membrane samples were measured by LC-MS/MS (Agilent Series 1290 LC, 6470A triple quadrupole mass spectrometer) using our standard methods [51]. Briefly, 20 µL of sample was injected onto a Waters XBridge BEH C18 (2.1×5 mm, 2.5 µm) guard column, and the 28 PFAS analytes were separated along a Waters XBridge BEH C18 column (2.1×150 mm, 2.5 µm). The column compartment temperature was maintained at 40 °C. The mobile phase was composed of (A) 10 mM NH₄Ac in LC-MS grade water and (B) 10 mM NH₄Ac in MeOH, and the gradient elution method was as follows: 0 to 3 min, 55% A, 45% B; ramp to 85% B for 6 min; ramp to 45% B for 1 min; and isocratic at 45% B for 6 min to re-equilibrate the column to initial conditions. The

mobile phase flow rate was set to 0.2 mL/min. The total method run time was 16 min. Negative mode electrospray ionization was applied for all targeted PFAS. Parent and fragment ions were scanned by dynamic multiple reaction monitoring with at least 15 scans acquired across the chromatographic peak for each PFAS. Results were analyzed through using the Agilent MassHunter Quantitative Analysis for QQQ software.

Dissolved organic carbon (DOC) concentrations were measured as non-purgeable organic carbon by a Shimadzu TOC-L analyzer (Shimadzu; Kyoto, Japan) calibrated with potassium hydrogen phthalate. Grab samples were diluted 50 \times and 100 \times to 20 mL with DI water before injection into the TOC-L analyzer.

2.3. Results and Discussion

Sorption isotherms were developed for PFAS uptake by the FAD-PET-75 membrane in solutions that replicated conditions in the Chesapeake Bay. Membrane coupons were added to 100-mL solutions that contained (i) 1-1000 $\mu\text{g L}^{-1}$ of individual PFAS and (ii) mixtures of over 20 PFAS at 100 $\mu\text{g L}^{-1}$ (each). For both cases, PFAS uptake was measured in solutions with (a) pH 5, 7, and 9, (b) 1, 10, and 100 mM of various salts, and (c) 1, 10, and 100 mg L^{-1} DOM (Table 2.2). All experiments were performed in triplicate at 20 $^{\circ}\text{C}$. The batch reactors were run for at least five days in HDPE bottles to reach equilibrium and minimize PFAS interactions with the container [49]. Then, PFAS and chloride concentrations were measured in the water and membrane phases and used to calculate selectivity coefficients using Eq. 2.1.

Based on prior work (not shown), temperature did not have a significant impact on the selectivity coefficients [51].

2.3.1. Impact of solution pH

Selectivity coefficients were calculated for each PFAS using Eq. 2.1. In Figure 2.1a, the selectivity coefficients are plotted against chain length, and the results revealed that selectivity coefficients increase as chain length increased. This trend was observed for all experimental conditions and attributed to the concomitant enhancement in hydrophobicity that accompanies an increase in the perfluoroalkyl chain length. The increased hydrophobicity of long-chain PFAS results in more hydrophobic-hydrophobic interactions with the polymer phase of the membrane, favoring sorption. The perfluoroalkane sulfonates (PFSA) exhibited greater selectivity than the perfluorocarboxylates (PFCA) and fluorotelomer sulfonates (FTS). PFSAs exhibited greater selectivity due to increased electrostatic and hydrophobic interactions with the fixed positively charged sites on the anion-exchange membrane. The sulfonate head group (SO_3^-) is more hydrophilic and more negatively charged compared to the carboxylate group (COO^-), allowing for stronger electrostatic interactions to occur [16], [52].

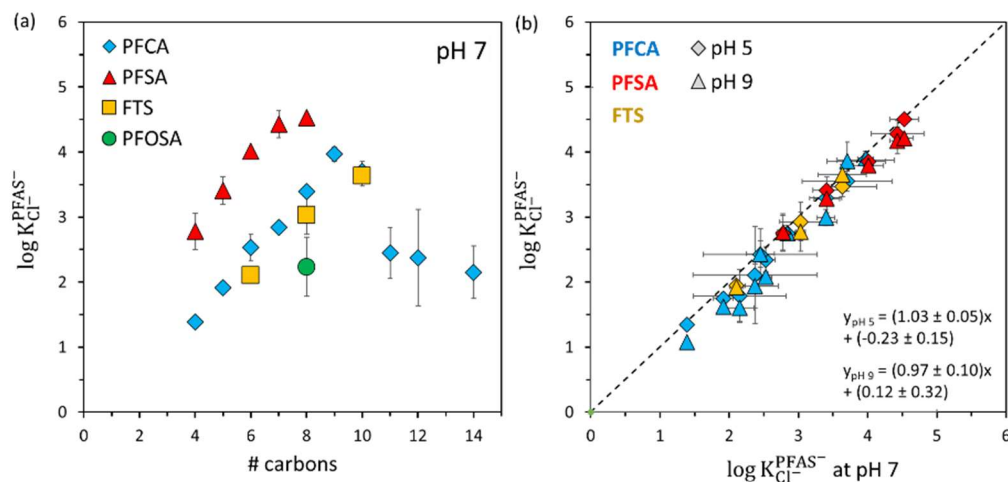


Figure 2.1. Selectivity coefficients for PFAS⁻ over Cl⁻ plotted as a function of (a) head group and chain length and (b) solution pH. Experimental conditions: 1×1 cm² FAD-PET-75 coupons initially in Cl⁻ form; 100 mL solution with 10 mM NaCl and PFAS at initial concentrations of 50, 100, 250, 500, and 1000 µg L⁻¹ (each); and 20 °C.

To determine the effect of solution pH on PFAS uptake by the membrane, batch tests were conducted at pH 5, 7, and 9. The selectivity coefficients measured at pH 5 and 9 were similar to those determined at pH 7 (Figure 2.1b). As a result, no significant differences were identified for the selectivity coefficients of perfluorocarboxylates, perfluoroalkane sulfonates, or fluorotelomer sulfonates at these pH levels. This outcome was explained by the speciation chemistry of PFAS, which primarily exist as anions in environmental water sources due to their low acid dissociation constants (*i.e.*, pK_a values) [53], [54]. This speciation chemistry was a major consideration in our decision to explore the use of anion-exchange membranes as passive samplers for the targeted PFAS.

Unlike the perfluorocarboxylates, perfluoroalkane sulfonates, and fluorotelomer sulfonates, the selectivity coefficients for PFAS with sulfonamide and sulfonamido

acetic acid moieties, namely PFOSA, N-MeFOSAA, and N-EtFOSAA, varied with pH (Figure 2.2). The pK_a values for these PFAS are environmentally relevant and range from 4 to 6 [54]. As a result, these compounds include neutral and anionic forms. At solution pH below the pK_a value, the protonated, neutral form of these PFAS is dominant. This pH-dependent speciation has implications for PFAS interactions with anion-exchange membranes. We hypothesized that the anionic form ($K_{Cl}^{PFAS^-}$) would exhibit higher selectivity than the neutral species (K_{Cl}^{H-PFAS}). Batch experiments were conducted at pH 2–12 to evaluate the hypothesis, and the corresponding data were fit to Eq. 2.2 by solving for the pK_a , K_{Cl}^{H-PFAS} , and $K_{Cl}^{PFAS^-}$ parameters. The model fits matched the experimental data (Figure 2.2), reinforcing the speciation-based corrections for selectivity coefficients of PFAS with environmentally relevant pK_a values. The solved parameters are listed in the figure. The calculated pK_a values were within range of previously reported values for PFOSA and slightly higher than estimates made from structure-based algorithms for N-EtFOSAA and N-MeFOSAA [54]. As the calculated pK_a of PFOSA was within the range of reported literature values, the speciation-based model was considered to be appropriate for implementing pH-based corrections for the selectivity coefficients for PFOSA and other compounds. For PFOSA, N-MeFOSAA, and N-EtFOSAA, Eq. 2.2 will be used in Eq. 2.1 to account for speciation effects on PFAS uptake by the passive sampler.

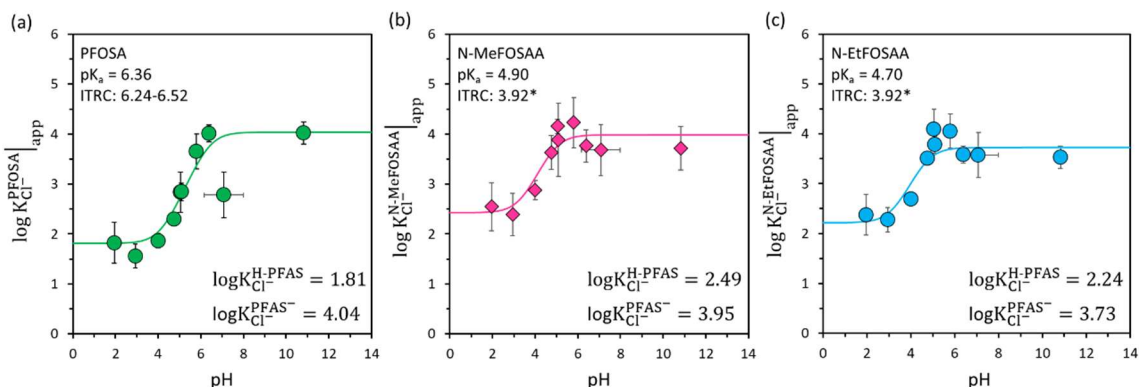


Figure 2.2. Selectivity coefficients for (a) PFOSA, (b) N-MeFOSAA, and (c) N-EtFOSAA over Cl^- at pH 2–12. The apparent selectivity coefficients were fit to Eq. 2.2. The calculated pK_a values were within the range of previously reported values for PFOSA but slightly higher than estimates from structure-based algorithms for N-EtFOSAA and N-MeFOSAA.

2.3.2. Impact of salt type and concentration

Real waters contain dissolved salts. This water quality parameter is especially important in the Chesapeake Bay estuary, which consists of freshwater in the upper reaches and seawater near the mouth [55], [56], [57]. To determine the impact of salt type and concentration on the selectivity coefficients of PFAS^- over Cl^- , experiments were conducted with sodium chloride (NaCl), sodium sulfate (Na_2SO_4), magnesium chloride (MgCl_2), calcium chloride (CaCl_2), potassium chloride (KCl), and sodium bicarbonate (NaHCO_3). Select data are included in this proposal to demonstrate the workflow and outcomes.

The selectivity coefficients measured in the presence of NaCl are shown in Figure 2.3. The compounds are arranged in order of hydrophobicity, according to the LC retention time on a C18 column. For hydrophilic, short-chain PFAS, the selectivity coefficients measured in solutions with 0.1–100 mM NaCl exhibited minor variations.

However, major differences were observed for the selectivity coefficients of the more hydrophobic, long-chain PFAS. This trend was observed for all salts, signifying the manifestation of salting-out effects on PFAS partitioning between the water and membrane phases.

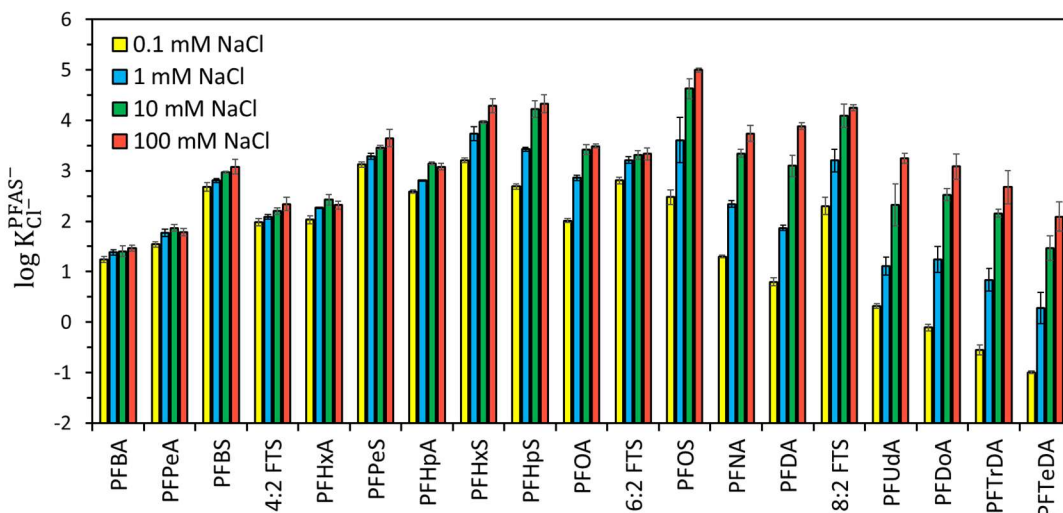


Figure 2.3. Selectivity coefficients for PFAS^- over Cl^- measured in the presence of variable NaCl. Experimental conditions: $1 \times 1 \text{ cm}^2$ FAD-PET-75 coupons initially in Cl^- form; 100 mL solution with nominal initial concentrations of $100 \mu\text{g L}^{-1}$ PFAS; pH 7; and 20°C .

The salting-out phenomenon is a process that increases the organization of water molecules in the system at high salt concentrations. As the salt concentration increases, the organization of water molecules around the salt ions increases the energetic costs of creating a cavity for other solutes. As a result, the equilibrium shifts toward the membrane phase, as the solute preferentially partitions into the membrane to compensate for the higher thermodynamic cost of dissolution [58], [59]. This phenomenon can be quantified by calculating Setschenow constants (K^S) for each PFAS-salt combination by fitting selectivity coefficients measured for variable salt

concentrations to Eq. 2.3-Eq. 2.4 (Figure 2.4a-b). The Setschenow constants can then be used to calculate the apparent selectivity coefficient as a function of salt concentration (Figure 2.4c). In brackish and saline waters, Eq. 2.4 will be used in Eq. 2.1 to account for salting-out effects on PFAS uptake by the passive sampler.

$$K_{\text{Cl}^-}^{\text{PFAS}^-} \big|_{\text{salt}} = 10^{(+K^S[\text{salt}])} K_{\text{Cl}^-}^{\text{PFAS}^-} \big|_{\text{DI}} \quad \text{Eq. 2.3}$$

$$K_{\text{Cl}^-}^{\text{PFAS}^-} \big|_{\text{salt}} = K_{\text{Cl}^-}^{\text{PFAS}^-} \big|_{10^{-1} \text{ M NaCl}} 10^{(+K^S[\text{salt}] - 10^{-1} K^S)} \quad \text{Eq. 2.4}$$

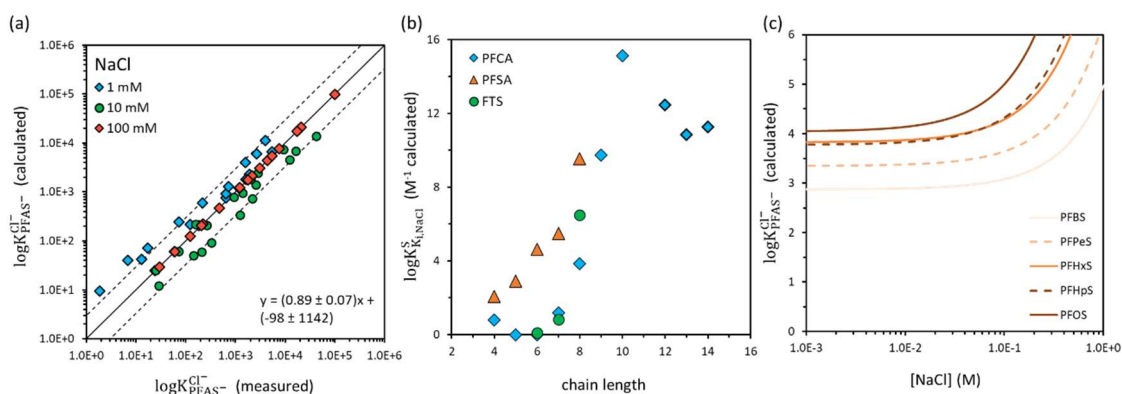


Figure 2.4. Solving for Setschenow constants: (a) calculated vs. measured selectivity coefficients for PFAS^- over Cl^- ; (b) calculated Setschenow constants for PFAS of concern; and (c) apparent selectivity coefficients for perfluoroalkane sulfonates (as representatives) as a function of NaCl concentration.

Selectivity coefficients recorded in the presence of 10 mM MgCl_2 and 10 mM CaCl_2 are plotted against those measured in solutions with 10 mM NaCl in Figure 2.5a. No significant differences were observed for the selectivity coefficients at this salt concentration, regardless of salt composition. Nevertheless, the selectivity coefficients differed at higher salt concentrations, and the impacts of those differences were captured by the corresponding Setschenow constants (Figure 2.5b). The

Setschenow constants for PFAS in solutions with MgCl_2 and CaCl_2 were considerably greater than those for solutions with NaCl . This outcome suggests that PFAS uptake by the anion-exchange membranes will be more selective in groundwaters containing high Mg^{2+} and Ca^{2+} concentrations, compared to surface water systems dominated by Na^+ .

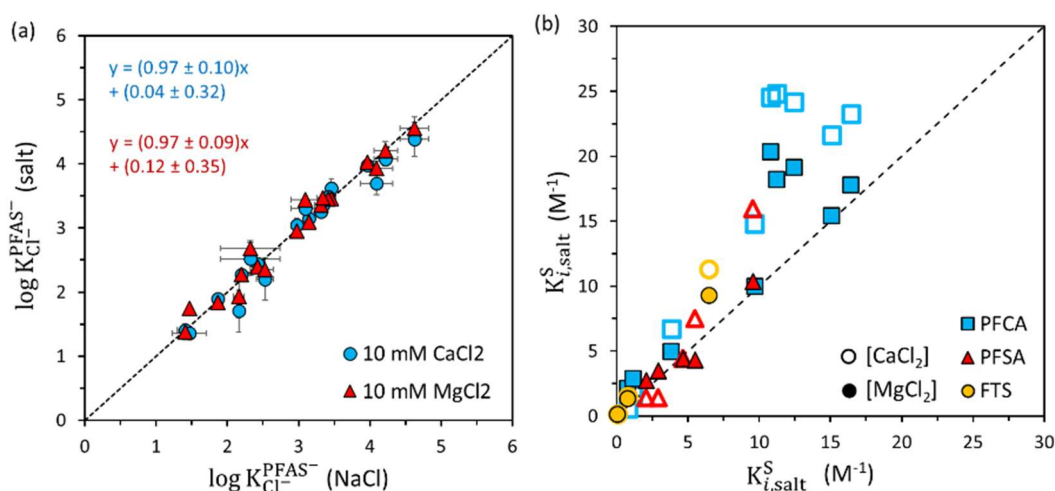


Figure 2.5. The (a) measured selectivity coefficients and (b) calculated Setschenow constants for PFCAs, PFSA, and FTSs. Data aligned with the 1:1 line in (a) indicate that salt type did not affect the apparent selectivity coefficients at salt concentrations of 10 mM; however, the data in (b) confirm that CaCl_2 and MgCl_2 exerted stronger salting-out effects than NaCl in more saline waters.

2.3.3. Impact of pH and salt concentration on the sulfonamide/o PFAS

As real waters may have variable pH and salinity, batch experiments were conducted to observe the combined effects of these two variables on the apparent selectivity coefficients for PFOSA, N-MeFOSAA, and N-EtFOSAA. Solutions with variable pH (*i.e.*, 2-11) and salt concentration (*i.e.*, 1, 10, and 100 mM NaCl) were tested in triplicate. The aqueous- and membrane-phase concentrations of PFAS^- and Cl^- were

determined, used to calculate the apparent selectivity coefficients (Eq. 2.1), and fit to Eq. 2.2 (Figure 2.6).

Similar to the results in Figure 2.2, speciation effects were evident from the observed effects of pH on the selectivity coefficients in Figure 2.6. In particular, the apparent selectivity coefficient was 1-3 orders of magnitude lower at $\text{pH} < 3$ than at $\text{pH} > 7$ for PFOSA, N-MeFOSAA, and N-EtFOSAA. This result stemmed from the lower prevalence of PFAS anions at acidic pH, preventing ion-exchange reactions with the fixed positive charges in the anion-exchange membrane. In addition, Figure 2.6 confirms the impact of salt concentration on the selectivity coefficients of the neutral ($K_{\text{Cl}^-}^{\text{H-PFAS}}$) and anionic ($K_{\text{Cl}^-}^{\text{PFAS}^-}$) PFAS molecules. This outcome agrees with findings from Figure 2.3, wherein salting-out phenomena increased the apparent selectivity coefficient in solutions with higher salt concentrations. Given the dual effects of pH and salt content, the aggregate data from Figure 2.6 were fit to Eq. 2.7 by solving for the "true" pK_a value and specific Setschenow constants for the protonated ($K_{\text{salt}}^{\text{S,H-PFAS}}$) and deprotonated species ($K_{\text{salt}}^{\text{S,PFAS}^-}$); these parameters are summarized in Table 2.3. The selectivity coefficients calculated from Eq. 2.7 were plotted against measured values in Figure 2.7, and the good fit of the modeled values to experimental data reinforced the universal calibration for PFAS uptake by the passive sampler in variable water quality conditions.

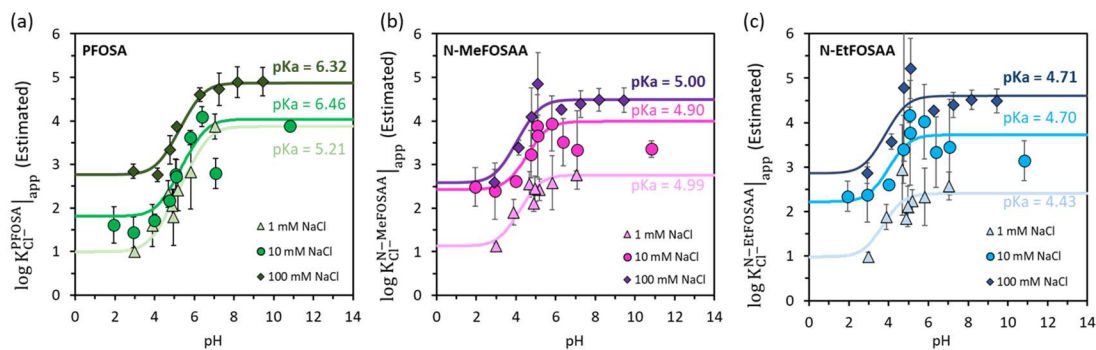


Figure 2.6. Apparent selectivity coefficients for (a) PFOSA, (b) N-MeFOSAA, and (c) N-EtFOSAA over Cl^- as a function of solution pH and salt concentration. Model curves were created by fitting the experimental data to Eq. 2.2. Experimental conditions: $1 \times 1 \text{ cm}^2$ FAD-PET-75 coupons initially in Cl^- form; 100 mL solution with 10 mM NaCl and PFAS at initial concentrations of 50, 250, and $500 \mu\text{g L}^{-1}$ (each) for $100 \mu\text{g L}^{-1}$ (in triplicate) for 1, 10, and 100 mM NaCl; and 20°C .

$$K_{\text{Cl}^-}^{\text{PFAS}^-} |_{\text{app}} = \left(1 + \frac{10^{-\text{pK}_a}}{10^{-\text{pH}}} \right)^{-1} K_{\text{Cl}^-}^{\text{H-PFAS}} |_{0.6 \text{ M NaCl}} 10^{(+K_{\text{salt}}^{\text{S,H-PFAS}} [\text{salt}] - 0.6 K_{\text{salt}}^{\text{S,H-PFAS}})} + \left(\frac{10^{-\text{pH}}}{10^{-\text{pK}_a}} + 1 \right)^{-1} K_{\text{Cl}^-}^{\text{PFAS}^-} |_{0.6 \text{ M NaCl}} 10^{(+K_{\text{salt}}^{\text{S,PFAS}^-} [\text{salt}] - 0.6 K_{\text{salt}}^{\text{S,PFAS}^-})}$$

Eq. 2.7

Table 2.3. Summary of the calculated "true" pK_a values and Setschenow constants for protonated and deprotonated PFAS used in Eq. 2.7.

Parameter	PFOSA	N-MeFOSAA	N-EtFOSAA
$K_{\text{salt}}^{\text{S,H-PFAS}}$	16.56	10.63	16.10
$K_{\text{salt}}^{\text{S,PFAS}^-}$	0.00	16.83	24.35
pK_a	6.49	5.66	4.75

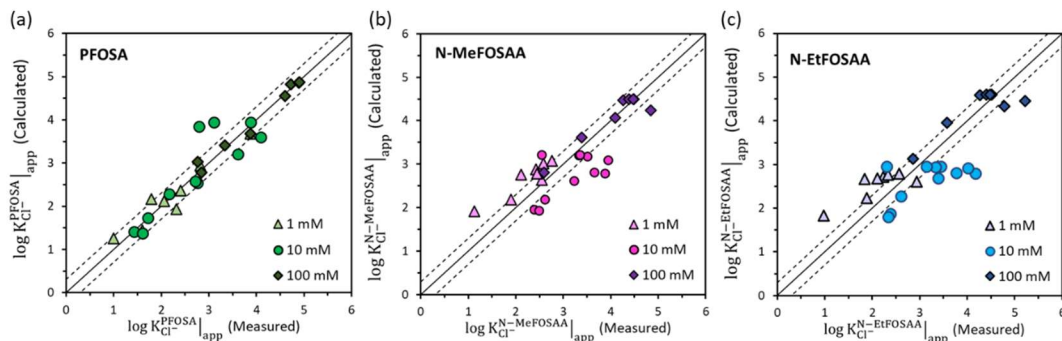


Figure 2.7. Selectivity coefficients for (a) PFOSA, (b) N-MeFOSAA, and (c) N-EtFOSAA over Cl^- calculated from Eq. 2.7 plotted against experimentally measured values. Experimental conditions: $1 \times 1 \text{ cm}^2$ FAD-PET-75 coupons initially in Cl^- form; 100 mL solution with 10 mM NaCl and PFAS at initial concentrations of 50, 250, and $500 \mu\text{g L}^{-1}$ (each) for $100 \mu\text{g L}^{-1}$ (in triplicate) for 1, 10, and 100 mM NaCl; and 20°C .

2.3.4 Impact of DOM type and content

DOM is a complex mixture of organic compounds that tend to display anionic characteristics in aquatic systems [60]. Therefore, DOM may compete with PFAS for binding sites on the anion-exchange membranes [35]. To investigate these effects, batch tests were conducted at initial DOM concentrations of 1 and 10 mg L^{-1} using natural organic matter (NOM) and two of the most abundant DOM subfractions, fulvic acids (FA) and humic acids (HA). FA molecules are smaller and more chemically reactive than HA compounds due to the greater proportion of oxygen-containing functional groups [61].

The selectivity coefficients for PFAS^- over Cl^- measured in the presence of NOM, FA, or HA and 10 mM NaCl are plotted against those measured in solutions with only 10 mM NaCl in Figure 2.1. No significant differences were observed for the selectivity coefficients measured in the presence of $1\text{--}10 \text{ mg L}^{-1}$ NOM. In contrast,

Figure 2.8b-c suggested a notable decrease in selectivity coefficients for long-chain PFAS for the experimental solutions that contained 1-10 mg L⁻¹ FA and HA. This observation was attributed to mass depletion of long-chain PFAS in these solutions, resulting in low aqueous-phase concentrations. The lower availability of these compounds increased the uncertainty associated with the calculated selectivity coefficients. [62], [63], [64].

To further assess the competition between DOM and PFAS, membrane-phase PFAS concentrations in the 10 mg L⁻¹ DOM solution were plotted against those from the 1 mg L⁻¹ DOM test (Figure 2.9). No significant differences were observed for the membrane-phase PFAS concentrations for solutions containing NOM and FA. In contrast, Figure 2.9c revealed that the membrane-phase PFAS concentrations decreased at higher HA concentrations, suggesting competitive adsorption effects or other mechanisms. For example, large HA may compete with PFAS from interacting with the quaternary amine ion-exchange sites [35], [65], [66], leading to lower PFAS uptake than expected in the absence of HA.

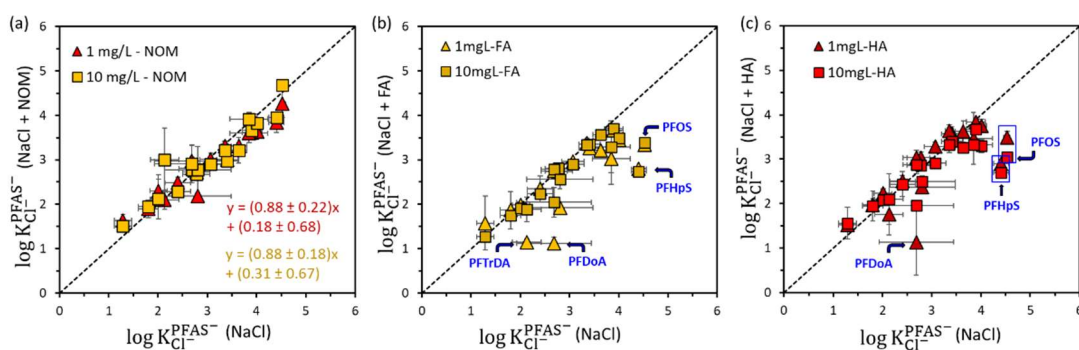


Figure 2.8. Measured selectivity coefficients for PFAS⁻ over Cl⁻ in solutions containing 1 and 10 mg L⁻¹ (a) DOM, (b) FA, and (c) HA plotted against those for solutions with no DOM, FA, or HA. Data deviating from the 1:1 line were

attributed to mass depletion of long-chain PFAS in the solution, increasing the uncertainty of the calculated selectivity coefficients.. All solutions contained 10 mM NaCl.

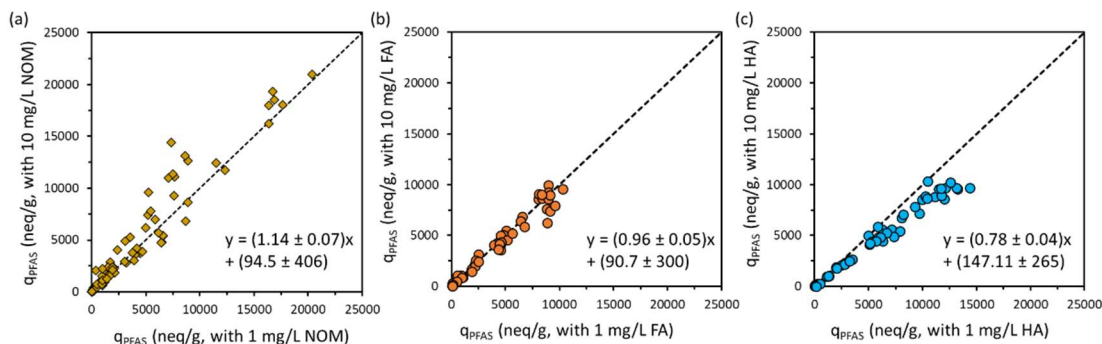


Figure 2.9. Membrane-phase PFAS concentrations for solutions with 1 and 10 mg L⁻¹ (a) DOM, (b) FA, and (c) HA. Data aligned with the 1:1 line indicate that the DOM content did not significantly affect the selectivity coefficient.

The above experiments were conducted to determine how individual water quality parameters affect the selectivity coefficient. From the preliminary results, we conclude: (i) pH has no effect on PFAS uptake for perfluorocarboxylates, perfluoroalkane sulfonates, and fluorotelomer sulfonates; (ii) the pH-dependent selectivity coefficients of PFAS with sulfonamide or sulfonamido acetic acid functional groups can be modeled using species-specific selectivity coefficients; (iii) selectivity coefficients increase in solutions with higher salt concentrations, and Setschenow constants can quantify these impacts; and (iv) DOM has negligible impacts on PFAS uptake, but waters with high HA content should be carefully evaluated before deployment of passive samplers. These findings were used to construct universal calibrations for our passive samplers.

2.4. Conclusions

The objectives of this chapter were to (1) measure the selectivity coefficients for PFAS⁻ over Cl⁻ and (2) develop models to accurately calculate selectivity coefficients for any water source. By conducting batch sorption experiments, varying solution pH, salt concentration, salt type, DOM concentration, and DOM type, we constructed a universal calibration that can be applied to accurately represent the selectivity coefficients for PFAS in any water type. The main findings for each water quality parameter are reported below. The overall universal calibration approach will be validated in the next chapter, which involves field deployment of our passive samplers in and around Baltimore Harbor.

We concluded that pH had a negligible impact on the selectivity coefficient for most PFAS due to the low pK_a values, which ensure the predominant presence of anionic species at environmentally relevant pH (*i.e.*, pH 5-9). For PFAS with environmentally relevant pK_a values (*e.g.*, PFOSA, N-MeFOSAA, and N-EtFOSAA), solution pH was a key parameter. Lower solution pH caused some of the PFAS to exist in neutral form, which interacted less favorably with the fixed positive charges in the anion-exchange membrane.

Salt concentration and salt type resulted in salting-out phenomena that exerted a strong influence on the magnitude of the selectivity coefficient, especially for long-chain PFAS. As salinity increased, the observed selectivity coefficient increased. These effects were quantified by calculating and applying Setschenow constants. Monovalent salts tended to exhibit similar Setschenow constants, suggesting NaCl

could serve as an appropriate surrogate. The Setschenow constants for divalent salts tended to be greater than those for NaCl, indicating the need for careful consideration of salting-out phenomena in hard water.

Minor impacts of DOM type and concentration were noted with respect to the selectivity coefficients of long-chain PFAS, but PFAS accumulation in the ion-exchange membranes did not significantly vary when the DOM concentration was varied. The observed differences in calculated selectivity coefficients for long-chain PFAS in the presence of DOM were attributed to mass depletion effects that increased uncertainty of the aqueous-phase PFAS concentrations at equilibrium. Importantly, negligible effects were observed for selectivity coefficients and membrane-phase PFAS concentrations in the presence of Suwannee River NOM; therefore, no adjustments were made to the universal calibration to account for DOM.

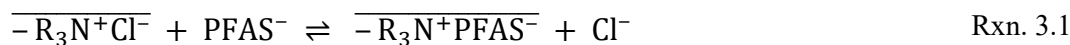
Chapter 3: Passive sampler field deployments to measure PFAS concentrations in and around Baltimore Harbor

3.1. Introduction

Major sources of per- and polyfluoroalkyl substances (PFAS) contamination include runoff from military bases that used aqueous film-forming foam (AFFF) and effluent from wastewater treatment facilities [7], [67]. While Maryland has initiated efforts to study PFAS within the state, data on PFAS levels in Baltimore Harbor remain scarce. As the Chesapeake Bay supports numerous communities that rely on its waters for sustenance, subsistence fishers are particularly vulnerable to PFAS exposure through the consumption of contaminated fish. In response to this risk, the Maryland Department of the Environment (MDE) issues fish consumption advisories for PFAS contamination when necessary [48]. With ongoing efforts to open Baltimore Harbor for public recreation, PFAS levels must be accurately quantified to assess potential risks to human health and environmental quality [68].

With assistance from Blue Water Baltimore, a non-governmental organization dedicated to restoring the quality of Baltimore's rivers, streams, and harbor, we conducted a sampling campaign at ten sites in Summer 2024. Through discussions with the Baltimore City Department of Public Works and a referral from Blue Water Baltimore to the Waterfront Partnership of Baltimore, we deployed passive samplers at a regional wastewater treatment plant and three trash wheels in Fall 2024 to (i) optimize and validate passive sampler performance and (ii) measure time-averaged PFAS concentrations at key locations in and around Baltimore Harbor. These tasks

required the use of the universal calibrations, reported in Chapter 2, that employ selectivity coefficients (modified versions of Eq. 3.1) to calculate time-averaged PFAS levels at the deployment sites.



$$K_{Cl}^{PFAS} = \frac{[PFAS^-]_{mem} [Cl^-]_{aq}}{[Cl^-]_{mem} [PFAS^-]_{aq}} \quad \text{Eq. 3.1}$$

3.2. Materials and Methods

3.2.1. Chemical reagents

PFAS certified standards, surrogates, and internal standards were obtained from Wellington Laboratories (Ontario, Canada). Bulk PFAS options were purchased from Fisher, Sigma, or Caymanchem, and the actual concentrations of stock solutions were determined against the certified standards. In total, 19 bulk PFAS, including 11 perfluorocarboxylic acids (*i.e.*, H-PFBA, H-PFPeA, H-PFHxA, H-PFHpA, H-PFOA, H-PFNA, H-PFDA, H-PFUdA, H-PFDoA, H-PFTrDA, H-PFTeDA), five perfluoroalkane sulfonate salts or perfluoroalkane sulfonic acids (*i.e.*, K-PFBS, Na-PFPeS, H-PFHxS, Na-PFHpS, Na-PFOS), three fluorotelomer sulfonate salts (*i.e.*, Na-4:2 FTS, Na-6:2 FTS, Na-8:2 FTS), and three perfluoroalkane sulfonamide or sulfonamido acetic acids (*i.e.*, H-PFOSA, H-N-MeFOSAA, H-N-EtFOSAA) were employed in laboratory experiments. Mixtures of nine mass-labeled surrogates (*i.e.*, H-M3PFBA, H-M4PFHpA, H-M8PFOA, H-MPFNA, H-MPFDoA, Na-MPFHxS, Na-M8PFOS, H-M8FOSA-I, H-d5-NEtFOSAA), and 15 mass-labeled internal standards (*i.e.*, H-MPFBA, H-M5PFPeA, H-MPFHxA, H-MPFOA, H-MPFDA, H-

MPFUdA, H-M2PFTeDA, Na-M3PFBS, Na-M3PFHxS, Na-MPFOS, Na-M2-4:2FTS, Na-M2-6:2 FTS, Na-M2-8:2FTS, H-M3HFPO-DA, H-d3-NMeFOSAA) were used to measure recovery efficiency and correct matrix effects, respectively. The full names of each PFAS standard and mass-labeled surrogate and internal standard are provided in Appendix A: Abbreviation Glossary along with salient physicochemical properties of each compound.

Other chemical reagents were procured from Fisher Scientific (Hampton, NH, USA). HPLC grade methanol (MeOH), acetonitrile, and ammonium acetate (NH₄Ac) were employed during solid-phase extraction (SPE) and solvent extraction of PFAS in water and membrane samples, respectively. Nitric acid (HNO₃) was applied to assist with digestion of membranes from field sampling campaigns involving passive samplers with copper mesh protective screens. LC-MS grade water, MeOH, and NH₄Ac were used during liquid chromatography with tandem mass spectrometry (LC-MS/MS). Deionized water was generated by a Neu-Ion System (Baltimore, MD, USA) for use during laboratory experiments and field sample processing.

3.2.2. Passive samplers

FAD-PET-75 anion-exchange membranes were purchased from the FuelCell Store (Bryan, TX, USA) for use as the active materials in the passive samplers deployed in laboratory experiments and field campaigns. Select properties of the FAD-PET-75 membranes are reported in Table 3.1.

Table 3.1 Physicochemical properties of the FAD-PET-75 anion-exchange membranes.

Membrane	Ion-exchange capacity (meq g ⁻¹)	Mass per area (mg cm ⁻²)	Standard thickness (μm)
FAD-PET-75	2.15 ± 0.15	7.75 ± 0.75	70 ± 10

For field deployment, the FAD-PET-75 membranes were incorporated into 3.7” (outer diameter) stainless-steel housings and protective mesh (Figure 3.1a). The size of the FAD-PET-75 membranes placed inside the passive samplers was usually 3×3 cm². An alternative sampler design incorporated a protective, antimicrobial copper mesh was also constructed and deployed in field campaigns (Figure 3.1.b) [69], [70].

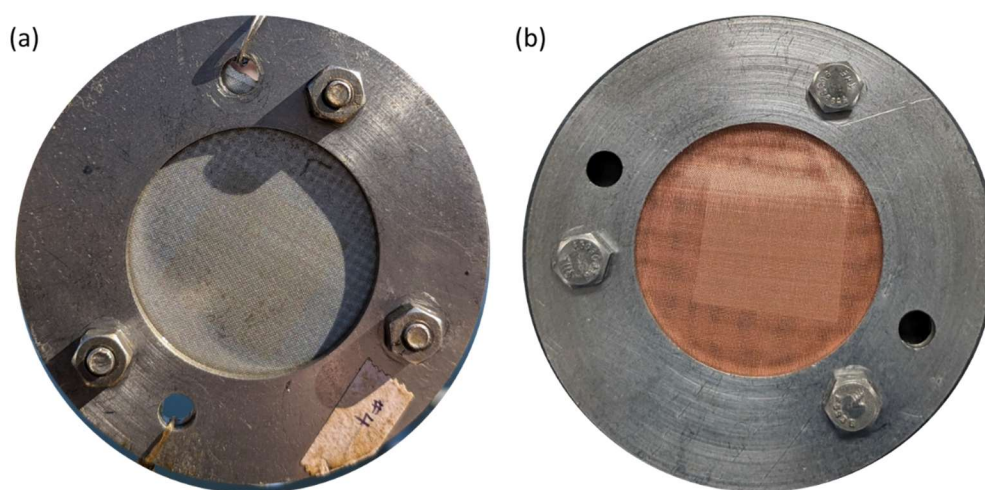


Figure 3.1 Passive sampler devices were constructed with protective (a) stainless-steel and (b) copper mesh and deployed in and around Baltimore Harbor.

3.2.3 Field sampling campaign

Based on discussions with Blue Water Baltimore, 10 sites in and around Baltimore Harbor were selected for collection of preliminary grab samples (Figure 3.2). Four sets of grab samples were collected over the span of four weeks in Summer 2024 and analyzed for PFAS concentrations (Section 3.4.1). These samples were used to establish a baseline for PFAS concentrations and composition in and around

Baltimore Harbor to inform the ideal locations for passive sampler deployment (Section 3.4.2). This initial assessment was crucial to understanding the potential contributions of wastewater effluent, stormwater, and other sources of PFAS to the Harbor [71].

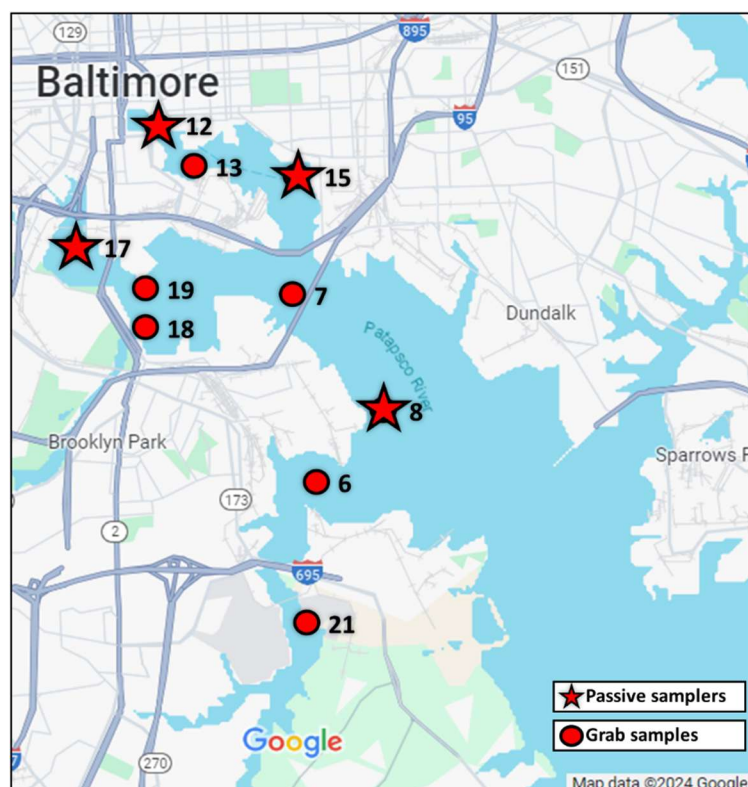


Figure 3.2. Map of sampling sites in and around Baltimore Harbor. Locations were selected with the help of Blue Water Baltimore to obtain samples with variable water quality and potential contamination sources.

3.2.4 PFAS analysis in grab samples from Baltimore Harbor

During sample collection, 500-mL HDPE bottles were submerged to at least 30 cm below the water surface and rinsed with surface water three times before being completely filled. A field blank, prepared with deionized water, was briefly opened and closed during the sampling campaign for quality assurance and quality control

purposes. The samples and field blank were placed in a cooler with ice packs and returned to the lab within two days. In the lab, each sample was spiked with 50 μL of a surrogate solution containing 50 $\mu\text{g L}^{-1}$ of nine mass-labeled PFAS to measure recovery efficiency during SPE. The spiked samples were loaded into pre-conditioned Oasis weak-anion exchange (WAX) SPE cartridges (6 cm^3 , 150 mg; Waters Corp; Milford, MA, USA). Recovery efficiencies were used to correct for PFAS losses during sample processing and determine the concentrations of targeted PFAS in each sample.

WAX cartridges were sequentially conditioned with 5 mL of (i) 0.1% NH_4Ac in MeOH and (ii) deionized water. When approximately 1 mL of deionized water remained in the cartridge, a sample, field blank, or laboratory blank was loaded to the SPE cartridge. The flow rate was adjusted to 1–3 mL min^{-1} by gravity or vacuum. After most of the sample volume was processed, the 500-mL container was sequentially rinsed with at least 2 mL of DI water and 50% methanol. The two rinsates were sequentially loaded to the SPE cartridge. The SPE manifold was vacuum-dried to remove any water or methanol residue from the cartridge. PFAS captured by the WAX cartridge were eluted into 10-mL HDPE test tubes with 5 mL of 5% NH_4Ac in acetonitrile. The eluates were dried at 50 $^{\circ}\text{C}$ under a gentle stream of nitrogen gas and reconstituted into 200 μL of 20 mM NH_4Ac in MeOH, 250 μL of DI water, and 50 μL of a 50 $\mu\text{g L}^{-1}$ mixture of 15 mass-labeled internal standards to correct for matrix effects during LC-MS/MS analysis (Section 3.1.6).

The 13 field blanks and 6 laboratory blanks were processed using the same procedures as the grab samples and then analyzed for the 28 PFAS analytes. For the field and laboratory blanks, 87% (461/532) of the measured PFAS concentrations were below the limit of detection, with the remainder of measurements (71/532) below the limit of quantitation. No PFAS were measured above the limit of quantitation in the field and laboratory blanks.

3.2.5. Passive sampler deployment and processing

Based on measured PFAS concentrations and composition in grab samples and ease of access to each site, passive samplers were deployed at three sites equipped with trash wheels that collect litter entering Baltimore Harbor. In particular, we partnered with the Baltimore Waterfront Partnership to deploy samplers at Mr. Trash Wheel (Baltimore Inner Harbor, mouth of the Jones Falls – Site 12 in Figure 3.1), Professor Trash Wheel (Baltimore Harbor, Canton neighborhood – Site 15 in Figure 3.1), and Gwynnda the Good Wheel of the West (Middle Branch of the Patapsco River, mouth of the Gwynns Falls – Site 17 in Figure 3.1). A sampler was also deployed in the effluent of an anonymous wastewater treatment plant (Site 8 in Figure 3.1) with permission from the Baltimore City Department of Public Works. Samplers were submerged at least 30 cm below the water surface and attached to (semi)permanent structures with stainless steel wire and nylon fishing line (Figure 3.3a). The samplers were deployed for periods of two, three, or four weeks in September – November 2024. During passive sampler deployment and retrieval, duplicate grab samples (Figure 3.3b) were also collected for analysis of PFAS concentrations (validation) and water quality parameters, including solution pH, salt concentration, and DOM content

(universal calibration). Other environmental conditions, such as recent rain events and algal blooms, were recorded during sample collection to help interpret the data.



Figure 3.3. Sample deployment and retrieval. (a) Passive samplers were tied to semi-permanent structures with stainless steel wire and nylon fishing line. Both options were used as a fail-safe in case either line was cut during deployments. (b) 500-mL grab samples (duplicate) were collected during passive sampler deployment and retrieval.

After retrieval, the passive samplers were disassembled, and the FAD-PET-75 membranes were removed, dried at 50 °C, and weighed. A preliminary analysis was conducted to optimize membrane processing methods. A 1×1 cm² section of the membrane was cut out, dried, and dissolved in 10 mL of HPLC-grade methanol (Figure 3.4). Some of the passive samplers equipped with a protective copper mesh developed an obvious copper scale on the membrane surface. In such cases, 10 µL of 70% HNO₃ was added to the methanolic extract to dissolve the scale and release any

PFAS bound to the copper oxide (Figure 3.4b). A 5 mL aliquot of the methanolic extract was diluted to 15 mL with DI water and spiked with 50 μL of a 50 $\mu\text{g L}^{-1}$ mixture of nine mass-labeled surrogates. Samples underwent SPE processing and reconstitution as outlined in Section 3.1.4 before LC-MS/MS analysis.

The full membrane analysis for passive samplers equipped with the protective stainless-steel mesh involved dissolving 2 \times 2 cm^2 coupons in 40 mL of 0.2 M NH_4Ac in MeOH. The membranes from samplers with protective copper mesh were processed by dissolving the full 3 \times 3 cm^2 coupons in 90 mL of 0.2 M NH_4Ac in MeOH with 10 μL of HNO_3 (Figure 3.4c); in this case, the entire membrane was used due to concerns of uneven PFAS loading onto the copper scale and membrane. A 10-mL aliquot of the methanolic extract was diluted to 40 mL with deionized (DI) water and processed in the same manner as the 1 \times 1 cm^2 membranes.



Figure 3.4. Passive sampler retrieval and processing. After retrieval, the passive samplers were cleaned and disassembled. Samplers with protective (a) stainless-steel mesh required less processing compared to the those using (b) copper mesh due to the absence of copper scale formed on the membrane during deployment. (c) MeOH digestion of $2 \times 2 \text{ cm}^2$ and $3 \times 3 \text{ cm}^2$ membrane coupons removed from the passive samplers with protective stainless-steel and copper meshes, respectively.

3.2.6. Analytical methods

PFAS concentrations in reconstituted extracts from the water and membrane samples were measured by LC-MS/MS (Agilent Series 1290 LC, 6470A triple quadrupole mass spectrometer) using our standard methods [51]. Briefly, $20 \mu\text{L}$ of sample was injected onto a Waters XBridge BEH C18 ($2.1 \times 5 \text{ mm}$, $2.5 \mu\text{m}$) guard column, and the 28 PFAS analytes were separated along a Waters XBridge BEH C18 column

(2.1×150 mm, 2.5 µm). The column compartment temperature was maintained at 40 °C. The mobile phase was composed of (A) 10 mM NH₄Ac in LC-MS grade water and (B) 10 mM NH₄Ac in MeOH, and the gradient elution method was as follows: 0 to 3 min, 55% A, 45% B; ramp to 85% B for 6 min; ramp to 45% B for 1 min; and isocratic at 45% B for 6 min to re-equilibrate the column to initial conditions. The mobile phase flow rate was set to 0.2 mL/min. The total method run time was 16 min. Negative mode electrospray ionization was applied for all targeted PFAS. Parent and fragment ions were scanned by dynamic multiple reaction monitoring with at least 15 scans acquired across the chromatographic peak for each PFAS. Results were analyzed through using the Agilent MassHunter Quantitative Analysis for QQQ software.

Background ions (*e.g.*, Cl⁻ and NO₃⁻) were measured by ion chromatography (IC; Thermo Scientific Dionex Integrion; Waltham, USA). Grab samples were diluted 50× and 100× with DI water before injection into the IC. Membrane samples were cut into 1×1 cm² coupons, dried, and dissolved in 10 mL of HPLC-grade methanol (Figure 3.4). A 2 mL aliquot of the methanolic extract was diluted to 5 mL with 3.75 mL DI water and 0.25 mL 1 M NaNO₃ before IC analysis.

Dissolved organic carbon (DOC) concentrations were measured as non-purgeable organic carbon by a Shimadzu TOC-L analyzer (Shimadzu; Kyoto, Japan) calibrated with potassium hydrogen phthalate. Grab samples were diluted 50× and 100× to 20 mL with DI water before injection into the TOC-L analyzer.

3.3. Results and Discussion

3.3.1. PFAS concentrations in grab samples from initial field campaign

Grab samples from the 10 sites in and around Baltimore Harbor contained 14 of the 28 targeted PFAS. The most prevalent PFAS included PFOS, PFHxA, PFPeA, PFHpA, and PFOA; note, PFOS and PFOA were included in the new EPA regulations with maximum contaminant levels of 4 ng L^{-1} for drinking water. In the Harbor, PFOS levels were consistently at or above the new regulation, with an average concentration of $3.81 \pm 1.18 \text{ ng L}^{-1}$ across all 41 grab samples. PFAS concentrations at each site were averaged from the four grab samples collected over the course of six weeks. Individual PFAS was then totaled across all sites are reported in Figure 3.5. The total PFAS concentrations varied by site, most likely due to differences in the contributing sources and degree of dilution. Site 15 in Figure 3.5, which is situated in the Canton area of Baltimore has a mostly residential community and a partial underground river (Harris Creek) feeding into the site, potentially explaining the relatively low total PFAS content (9 ng L^{-1}). In contrast, 19.5 ng L^{-1} of PFAS were measured at Site 8 in Figure 3.4, which was located at the effluent pipe of a wastewater treatment plant; many previous studies have confirmed wastewater to be a source of PFAS [8], [67], [71].

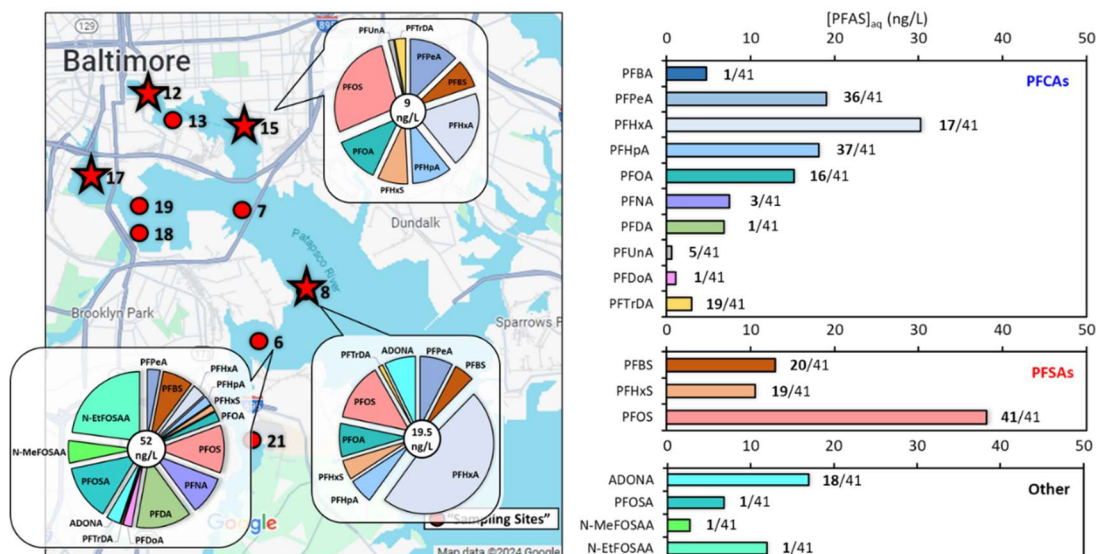


Figure 3.5. Total PFAS concentrations detected in preliminary grab samples. The detection frequency for each PFAS is indicated at the end of the bars in the right panel for the 41 grab samples.

3.3.2. Optimization of passive sampler design

The initial passive samplers deployed at the three Trash Wheels included a protective copper mesh. As shown in Figure 3.4b, the copper mesh oxidized during deployment in the brackish water present at Mr. Trash Wheel and Prof. Trash Wheel, leading to formation of a copper scale on the membrane. The passive sampler deployed at the more freshwater site, Gwynnda Trash Wheel, did not experience copper oxidation, confirming that salinity played a role in the observed oxidation [72]. During membrane digestion, the membrane polymer appeared to be completely dissolved, but the copper scale remained. The presence of the copper scale on the membrane raised a concern of additional PFAS uptake onto the surface of copper particles, which would decrease the accuracy of our universal calibration. The main mechanisms for PFAS interacting with the copper scale involve electrostatic interactions and ternary complexation. For example, previous studies reported that metal cations can

neutralize PFAS negative charges, enhance hydrophobic interactions, and facilitate PFAS adsorption to surfaces [73]. Metal ions, like copper II, can also form ternary complexes with PFAS and surfaces to enhance adsorption [74]. To ensure accurate PFAS analysis from the membrane and copper scale, 10 μL of HNO_3 was added to the digestate to dissolve the copper scale and release any PFAS [50]. Samples were processed with SPE and reconstituted for LC-MS/MS analysis.

In Figure 3.6, the PFAS mass on membranes included in passive samplers containing the stainless-steel mesh is plotted against that with the copper mesh for two- and three-week deployments. Many of the data points fell below the 1:1 line, indicating greater uptake of PFAS on the membrane contained within the passive sampler with the copper mesh. These results confirm our concerns that the copper scale accumulated PFAS, rendering our universal calibration inaccurate. Given this outcome, the remaining deployments employed passive samplers with a stainless-steel mesh to prevent any physical damage to or biological growth on the membrane (Figure 3.4a).

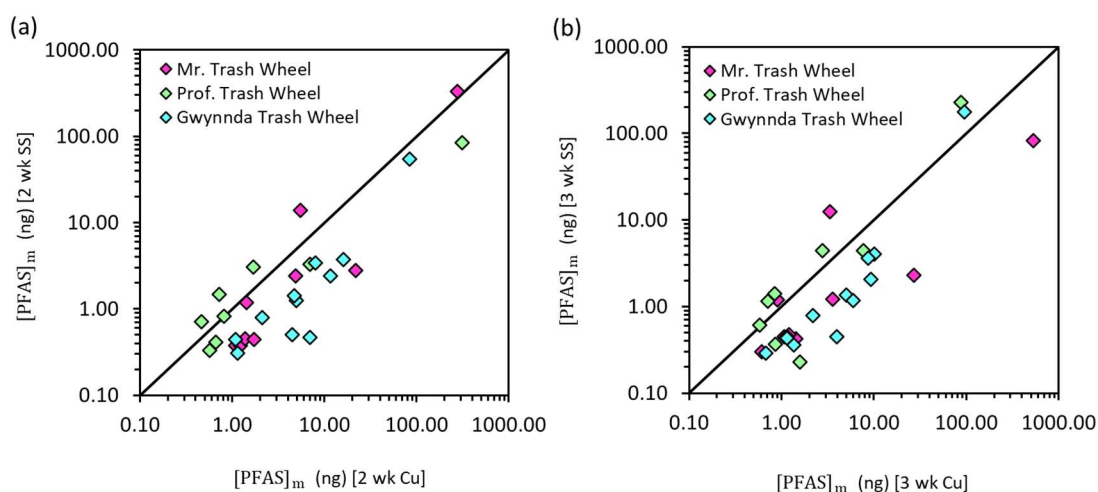


Figure 3.6. Comparison of PFAS mass accumulated in passive samplers with stainless-steel and copper protective mesh during (a) two- and (b) three-week deployments. Regression analysis of the complete dataset yielded the following relationships: (a) $\log [\text{PFAS}]_{\text{m,SS}} = (0.82 \pm 0.08) \log [\text{PFAS}]_{\text{m,Cu}} - (0.21 \pm 0.06)$, and (b) $\log [\text{PFAS}]_{\text{m,SS}} = (0.87 \pm 0.09) \log [\text{PFAS}]_{\text{m,Cu}} - (0.20 \pm 0.07)$. Because the slope of the trendlines was less than 1, significantly more PFAS accumulated in the presence of the copper mesh.

3.3.3. Evaluation of required deployment time

Because our passive samplers are calibrated according to equilibrium, the deployment time is an important variable. If the samplers do not reach equilibrium, then the universal calibration will not be accurately applied. To evaluate this issue, samplers were deployed at the three Trash Wheels and wastewater effluent for two, three, and four weeks. Figure 3.7 confirms that no differences were observed in the total PFAS mass accumulated in the samplers for the two-, three-, and four-week deployment periods. This outcome indicated that the sampler reached equilibrium within two weeks of deployment at these sites. While shorter deployment periods may also be appropriate, this aspect will be further evaluated in future studies.

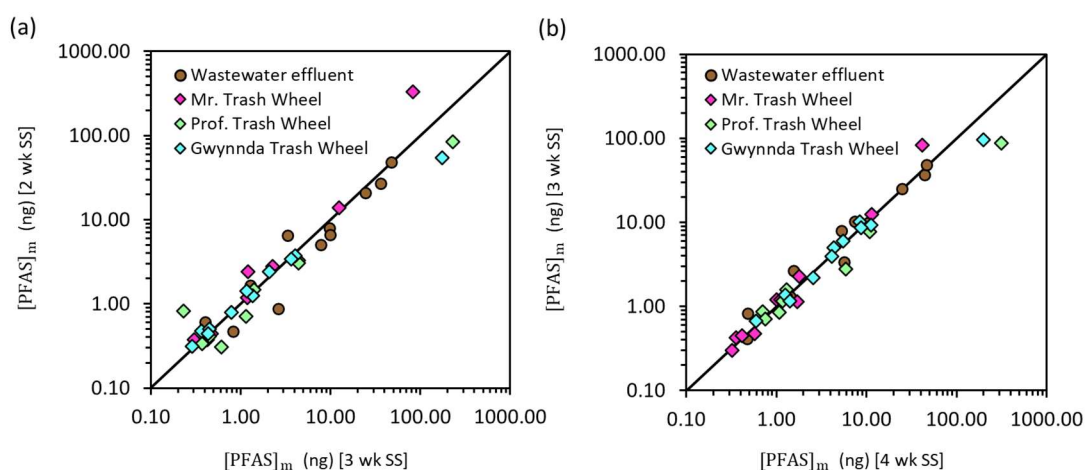


Figure 3.7. Comparison of PFAS mass accumulated on the membrane for (a) two- and three-week deployments and (b) three- and four-week deployments. All

data correspond to the passive samplers equipped with protective stainless-steel meshes. Regression analysis of the complete dataset yielded the following relationships: (a) $\log [\text{PFAS}]_{\text{m},2\text{wk}} = (0.92 \pm 0.04) \log [\text{PFAS}]_{\text{m},3\text{wk}} + (0.004 \pm 0.03)$, and (b) $\log [\text{PFAS}]_{\text{m},3\text{wk}} = (0.93 \pm 0.03) \log [\text{PFAS}]_{\text{m},4\text{wk}} + (0.01 \pm 0.02)$. Because the slope of the trendlines were close to 1 and the intercepts overlapped with 0, no significant differences in PFAS accumulation were identified between the two-, three-, and four-week deployments.

3.3.4. Calculation of time-averaged PFAS levels at field sites

The mass composition of PFAS accumulated in the passive samplers was measured for each site and plotted in Figure 3.8. The PFAS distribution was similar for samplers deployed at the three Trash Wheels, but key differences were noted for the passive samplers placed in wastewater effluent. For all sites, PFOS constituted most of the PFAS mass accumulated onto the membrane. This outcome was attributed to (i) higher PFOS levels in the water sources (Figure 3.4) and (ii) the higher selectivity coefficient of PFOS compared to other targeted PFAS (Figure 2.1). At the Trash Wheel locations, PFOA and PFHxA were the next most prevalent PFAS, whereas 6:2 FtS and PFBS were predominant in wastewater effluent. These differences suggest variable sources or fate and transport of PFAS at the sampling locations [75]. Nevertheless, the variable PFAS uptake and composition reinforce the ability of our passive sampler to capture diverse PFAS in different water sources.

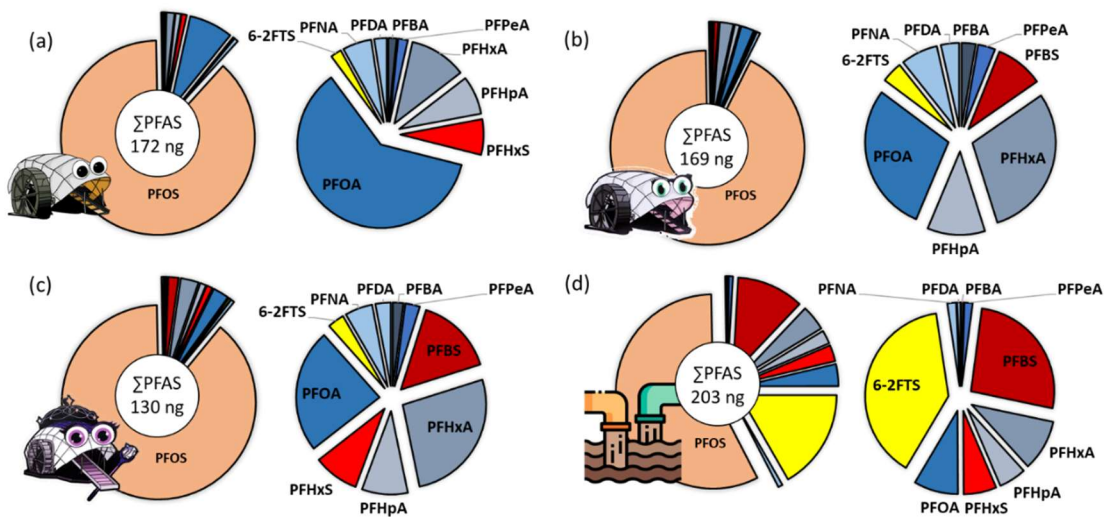


Figure 3.8. Mass and composition of PFAS accumulated on the passive samplers deployed at (a) Mr. Trash Wheel, (b) Prof. Trash Wheel, (c) Gwynnda Trash Wheel, and (d) wastewater effluent. Note, the secondary pie charts show all PFAS except PFOS.

When applying the universal calibration to our samplers, the main parameter that needed correction was salt concentration due to the general absence of PFOSA, N-MeFOSAA, and N-EtFOSAA (pH-based effects, Figure 2.2) in the samplers and the negligible impacts of DOM on the calibration (Figure 2.8). Clear salinity gradients were observed from more upstream (*e.g.*, Gwynnda Trash Wheel) to farther downstream sites (*e.g.*, Prof. Trash Wheel) located in and around Baltimore Harbor (**Table 3.2**). The water in the Harbor was also more brackish than wastewater effluent. By measuring the membrane-phase PFAS^- concentration and the Cl^- concentrations in the membrane and aqueous phases, the salinity-corrected selectivity coefficient (Eq. 3.2) was used to calculate the time-averaged PFAS concentrations in water from each site using Eq. 3.1.

$$K_{\text{Cl}^-}^{\text{PFAS}^-} \big|_{\text{salt}} = K_{\text{Cl}^-}^{\text{PFAS}^-} \big|_{0.6 \text{ M NaCl}} 10^{(+K^{\text{S}}[\text{salt}] - 0.6 K^{\text{S}})} \quad \text{Eq. 3.2}$$

Table 3.2. The water quality conditions at each sampling location. These parameters will be used in tandem with our universal calibration to calculate the time-averaged PFAS concentration in the aqueous phase according to the measured PFAS and Cl^- levels in the membrane.

Site	pH	Chloride (mM)
Wastewater effluent	7.38 ± 0.16	3.35 ± 0.47
Mr. Trash Wheel	7.65 ± 0.32	37.9 ± 14.8
Prof. Trash Wheel	7.33 ± 0.02	111 ± 27
Gwynnda Trash Wheel	7.58 ± 0.20	33.3 ± 18.5

Below, an example back-calculation is reported for clarity. During the three-week deployment of the passive sampler at Mr. Trash Wheel, the measured water quality parameters included 40.15 mM Cl^- in the aqueous phase and 0.89 meq/g Cl^- in the membrane phase. The measured PFOS concentration in the membrane was 1.36×10^4 ng/g. From Chapter 2, the Setschenow constant for PFOS was 1.15, and the selectivity coefficient for PFOS over Cl^- was 3.15×10^5 at the reference salt concentration (0.6 M NaCl). As pH exhibits no impact on the selectivity coefficient for PFOS over Cl^- , Eq. 3.2 was used to determine the salt-corrected selectivity coefficient. By substituting the relevant values into Eq. 3.3.1, the selectivity coefficient for PFOS at Mr. Trash Wheel was determined (Eq. 3.3.2). This salinity-corrected selectivity coefficient was integrated into Eq. 3.3.3 to calculate the time-averaged PFAS concentration in the water at Mr. Trash Wheel over the three-week deployment period (Eq. 3.3.4). The corresponding value was 8.50 ng/L, approximately 100% greater than the new EPA drinking water regulation for PFOS.

$$K_{\text{Cl}^-}^{\text{PFOS}^-} \big|_{\text{salt}} = K_{\text{Cl}^-}^{\text{PFOS}^-} \big|_{0.6 \text{ M NaCl}} 10^{(+K^S[\text{salt}] - 0.6 K^S)} \quad \text{Eq. 3.3.1}$$

$$K_{Cl^-}^{PFOS^-}|_{salt} = (3.15 \times 10^5) 10^{((1.15)(0.04 \text{ M } Cl^-) - 0.6 (1.15))}$$

$$= 7.20 \times 10^4$$
Eq. 3.3.2

$$K_{Cl}^{PFOS} = \frac{[PFOS^-]_{mem} [Cl^-]_{aq}}{[Cl^-]_{mem} [PFOS^-]_{aq}}$$
Eq. 3.3.3

$$[PFOS^-]_{aq} = \frac{[PFOS^-]_{mem} [Cl^-]_{aq}}{[Cl^-]_{mem} K_{Cl}^{PFOS}} = \frac{\left(1.36 \times 10^4 \frac{ng}{g}\right) \left(40.15 \frac{meq}{L}\right)}{\left(0.89 \frac{meq}{g}\right) (7.20 \times 10^4)}$$

$$= 8.50 \frac{ng}{L}$$
Eq. 3.3.4

The performance of the passive sampler was evaluated by comparing the time-averaged, aqueous-phase PFAS concentrations to the range of PFAS concentrations measured in four grab samples collected across the deployment campaign. Most of the data in **Figure 3.9** fall within one order magnitude of the 1:1 line, indicating that our in-lab calibration was able to successfully correct for the water quality parameters of each site. Data points farther away from the 1:1 line were mostly associated with measurements at Prof. Trash Wheel and Gwynnda Trash Wheel. Several reasons could have caused these deviations. First, Prof. Trash Wheel is situated in an area that is more tidally influenced, where complex dynamic processes may be occurring to affect not only PFAS concentrations but also Cl^- levels that influence our universal calibration. Gwynnda Trash Wheel is located next to the Baltimore City solid waste incinerator and at the mouth of the Gwynns Falls, which is known to have wastewater inputs due to sanitary sewer leaks and overflows [76], [77], [78], [79]. These factors could influence PFAS inputs at these sites. Furthermore, the dynamic hydrological conditions at these sites may greatly influence the range of PFAS concentrations in grab samples; therefore, agreement between the passive sampler-based concentrations and those from grab samples is not necessarily expected or desired. The key

advantage of passive samplers is the ability to determine time-averaged concentrations that better represent long-term PFAS levels in Baltimore Harbor. Notably, PFAS concentrations measured in wastewater effluent were more similar for the passive samplers and grab samples, which may reinforce the dynamic conditions of the Harbor relative to more stable PFAS levels in wastewater effluent.

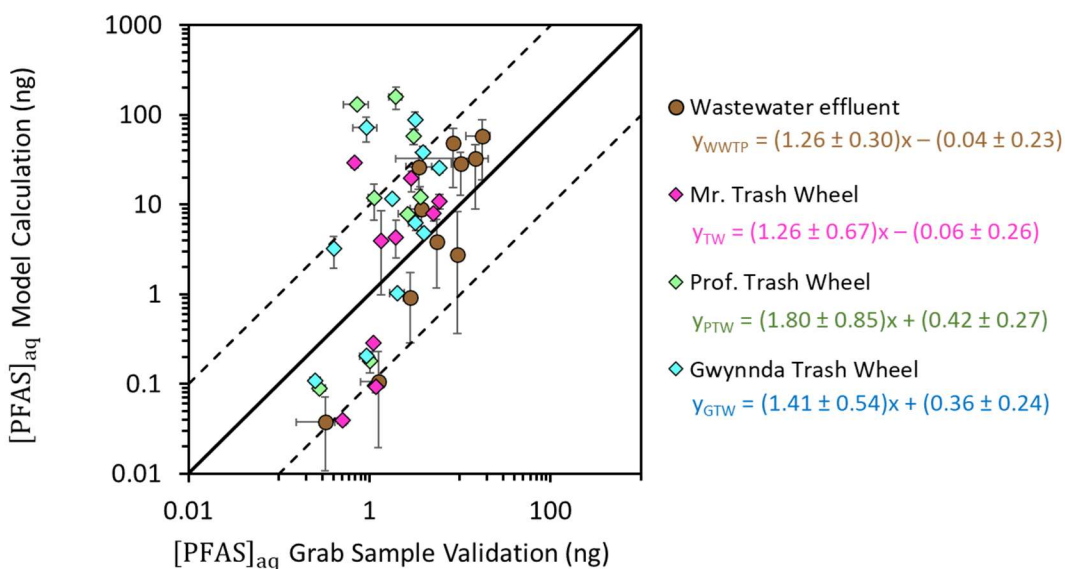


Figure 3.9. PFAS concentrations determined from passive samplers plotted against those measured in grab samples. The dashed lines are one order of magnitude away from the solid 1:1 line. Regression analysis of the complete dataset yielded the following relationships shown. Because the slope of the trendlines were close to 1 and the intercepts overlapped with 0, no significant differences in aqueous PFAS concentration were identified between the grab samples and the passive sampler calculations.

3.4. Conclusions

The objective of this chapter was to deploy passive samplers into real water sources and employ the universal calibration constructed in Chapter 2 to determine PFAS concentrations in and around Baltimore Harbor. Four sites were chosen for passive sampler deployment with assistance from Blue Water Baltimore, the Waterfront

Partnership, and the Baltimore Department of Public Works. The initial passive sampler deployments enabled optimization of the protective mesh material and length of deployment. In particular, the copper mesh resulted in formation of a copper scale on the membrane, resulting in an additional PFAS adsorption mechanism that was not accounted for in the universal calibration. As a result, a stainless-steel protective mesh was implemented into the samplers. The passive samplers were deployed for two, three, and four weeks, but no major changes in PFAS accumulation were observed after two weeks. As such, we determined that the passive samplers should be deployed for at least two weeks. The universal calibration constructed in Chapter 2 was applied to the passive samplers to calculate the time-averaged, aqueous-phase concentrations of PFAS at each site. The long-term, time-averaged PFAS levels determined by the passive samplers were generally within one order of magnitude of PFAS concentrations measured in grab samples, which are more influenced by dynamic conditions. This outcome was considered highly successful, demonstrating the promise of anion-exchange membrane based passive samplers with universal calibration to measure PFAS in diverse water sources.

Chapter 4: Conclusion

Overall conclusions

4.1. Water quality impacts on PFAS selectivity coefficients for the development of a universal calibration

Chapter 2 aimed to (1) determine the selectivity coefficients for PFAS⁻ over Cl⁻ and (2) develop predictive models to accurately calculate selectivity coefficients across various water sources. Batch sorption experiments were conducted to assess the effects of solution pH, salt concentration, salt type, DOM concentration, and DOM type on the selectivity coefficients. Results were then used to develop a universal calibration that can accurately represent the selectivity coefficients of PFAS across different water types. The main findings for each water quality parameter are reported below.

We concluded that pH had a negligible impact on the selectivity coefficient for most PFAS due to their low pK_a values, which ensure the predominance of anionic species at environmentally relevant pH levels (*i.e.*, pH 5-9). However, for PFAS with environmentally relevant pK_a values (*e.g.*, PFOSA, N-MeFOSAA, N-EtFOSAA), solution pH plays a crucial role. Lower solution pH caused some of the PFAS to exist in their neutral form, which interacted less favorably with the fixed positive charges in the anion-exchange membrane.

Salt concentration and type experiments observed the significant impact of salting-out phenomena on the selectivity coefficient's magnitude, particularly for long-chain

PFAS. As salinity increased, the observed selectivity coefficient also increased. These effects were quantified by calculating and applying Setschenow constants.

Monovalent salts generally exhibited similar Setschenow constants, suggesting that NaCl could serve as an appropriate representative. In contrast, the Setschenow constants for divalent salts were typically greater than those for NaCl, highlighting the importance of carefully considering salting-out effects in hard water.

The combined effects of pH and salinity confirmed that the trends observed in single-variable experiments remained valid when these factors were applied simultaneously. Higher apparent selectivity coefficients were observed at elevated salt concentrations and at higher pH for PFAS containing sulfonamide or other similar functional groups.

Minor impacts of DOM type and concentration were observed concerning the selectivity coefficients of long-chain PFAS. However, PFAS accumulation in the ion-exchange membranes did not vary significantly with changes in DOM concentration. The observed differences in calculated selectivity coefficients for long-chain PFAS in the presence of DOM were attributed to mass depletion effects, which increased the uncertainty of the aqueous-phase PFAS concentrations at equilibrium. Notably, as negligible effects were observed on selectivity coefficients and membrane-phase PFAS concentrations in the presence of Suwannee River NOM, no adjustments were made to the universal calibration to account for DOM.

4.2. Passive sampler field-validations utilizing the constructed universal calibration

Chapter 3 aimed to deploy passive samplers in real water sources and apply the universal calibration developed in Chapter 2 to quantify PFAS concentrations in and

around Baltimore Harbor. Four deployment sites were selected in collaboration with Blue Water Baltimore, the Waterfront Partnership of Baltimore, and the Baltimore City Department of Public Works. Initial deployments facilitated the optimization of both the protective mesh material and length of deployment. The use of copper mesh led to the formation of a copper scale on the membrane, introducing an unintended PFAS adsorption mechanism that was not accounted for in the universal calibration. As a result, stainless-steel mesh was adopted in subsequent deployments.

Passive samplers were deployed for durations of two, three, and four weeks, with no significant differences in PFAS accumulation observed beyond two weeks. Therefore, we determined that the passive sampler should be deployed for a minimum of two weeks. The universal calibration model from Chapter 2 was then applied to estimate time-averaged, aqueous-phase PFAS concentrations at each site. The PFAS concentrations measured by the passive samplers were generally within one order of magnitude of those obtained from grab samples, which are more susceptible to dynamic environmental variability. This alignment highlights the effectiveness of anion-exchange membrane-based passive samplers with universal calibration as a reliable method for measuring PFAS in diverse aquatic environments.

4.3. Raising awareness of PFAS contamination in the harbor through the dissemination of information to collaborators

Field deployments at the trash wheels and wastewater treatment plant were made possible through the collaboration and support of Blue Water Baltimore, the Waterfront Partnership, and the Baltimore Department of Public Works. Given their

instrumental role in facilitating site access and logistical coordination, the findings from this study will be shared with these organizations. This dissemination will not only enhance local understanding of PFAS contamination but also support ongoing environmental monitoring and policy development efforts aimed at improving water quality in Baltimore Harbor. Furthermore, sharing these results may inform future sampling strategies and remediation initiatives, fostering continued collaboration between researchers and community stakeholders.

4.4. Future work

Further development of this novel passive sampler will be undertaken to enhance its performance and applicability. In particular, efforts will focus on refining the universal calibration by testing additional common salts (*e.g.*, sodium bicarbonate, sodium sulfate) and more complex salt mixtures. Moreover, expanded field deployments will be carried out across a range of environments to evaluate sampler effectiveness not only in surface water, but also in pore water and sediment matrices.

Appendices

Appendix A: Abbreviation Glossary

Perfluorocarboxylates (PFCAs):

Perfluorobutanoic acid (PFBA), perfluoropentanoic acid (PFPeA), perfluorohexanoic acid (PFHxA), perfluoroheptanoic acid (PFHpA), perfluorooctanoic acid (PFOA), perfluorononanoic acid (PFNA), perfluorodecanoic acid (PFDA), perfluoroundecanoic acid (PFUdA), perfluorododecanoic acid (PFDoA), perfluorotridecanoic acid (PFTrDA), perfluorotetradecanoic acid (PFTeDA)

Perfluoroalkane sulfonates (PFSAAs):

Perfluorobutane sulfonate (PFBS), perfluoropentane sulfonic acid (PFPeS), perfluorohexane sulfonate (PFHxS), perfluoroheptane sulfonic acid (PFHpS), perfluorooctane sulfonic acid (PFOS)

Fluorotelomer Sulfonates (FTS):

4:2 fluorotelomer sulfonate (4:2 FTS), 6:2 fluorotelomer sulfonate (6:2 FTS), 8:2 fluorotelomer sulfonate (8:2 FTS)

Perfluoroalkane sulfonamide and sulfonamido acetic acid:

Perfluorooctanesulfonamide (PFOSA), N-Methylperfluorooctane sulfonamidoacetic acid (N-MeFOSAA), N-ethyl perfluorooctane sulfonamido acetic acid (N-EtFOSAA).

Replacement PFAS:

Hexafluoropropylene oxide dimer acid (HFPO-DA)

Bibliography

- [1] K. M. Rodgers, C. H. Swartz, J. Occhialini, P. Bassignani, M. McCurdy, and L. A. Schaider, "How Well Do Product Labels Indicate the Presence of PFAS in Consumer Items Used by Children and Adolescents?," *Environ. Sci. Technol.*, vol. 56, no. 10, pp. 6294–6304, May 2022, doi: 10.1021/acs.est.1c05175.
- [2] O. US EPA, "Per- and Polyfluoroalkyl Substances (PFAS)." Accessed: Jul. 02, 2024. [Online]. Available: <https://www.epa.gov/sdwa/and-polyfluoroalkyl-substances-pfas>
- [3] R. C. Buck *et al.*, "Perfluoroalkyl and polyfluoroalkyl substances in the environment: Terminology, classification, and origins," *Integrated Environmental Assessment and Management*, vol. 7, no. 4, pp. 513–541, 2011, doi: 10.1002/ieam.258.
- [4] F. Li *et al.*, "A concentrate-and-destroy technique for degradation of perfluorooctanoic acid in water using a new adsorptive photocatalyst," *Water Research*, vol. 185, p. 116219, Oct. 2020, doi: 10.1016/j.watres.2020.116219.
- [5] M. M. Lorah *et al.*, "Anaerobic biodegradation of perfluorooctane sulfonate (PFOS) and microbial community composition in soil amended with a dechlorinating culture and chlorinated solvents," *Science of The Total Environment*, vol. 932, p. 172996, Jul. 2024, doi: 10.1016/j.scitotenv.2024.172996.
- [6] Y. Zhu, H. Ji, K. He, L. Blaney, T. Xu, and D. Zhao, "Photocatalytic degradation of GenX in water using a new adsorptive photocatalyst," *Water Research*, vol. 220, p. 118650, Jul. 2022, doi: 10.1016/j.watres.2022.118650.
- [7] D. Q. Andrews, J. Hayes, T. Stoiber, B. Brewer, C. Campbell, and O. V. Naidenko, "Identification of point source dischargers of per- and polyfluoroalkyl substances in the United States," *AWWA Water Science*, vol. 3, no. 5, p. e1252, 2021, doi: 10.1002/aws2.1252.
- [8] S. Kurwadkar *et al.*, "Per- and polyfluoroalkyl substances in water and wastewater: A critical review of their global occurrence and distribution," *Science of The Total Environment*, vol. 809, p. 151003, Feb. 2022, doi: 10.1016/j.scitotenv.2021.151003.
- [9] D. Salvatore *et al.*, "Presumptive Contamination: A New Approach to PFAS Contamination Based on Likely Sources," *Environ. Sci. Technol. Lett.*, vol. 9, no. 11, pp. 983–990, Nov. 2022, doi: 10.1021/acs.estlett.2c00502.
- [10] N. M. Brennan, A. T. Evans, M. K. Fritz, S. A. Peak, and H. E. von Holst, "Trends in the Regulation of Per- and Polyfluoroalkyl Substances (PFAS): A Scoping Review," *International Journal of Environmental Research and Public Health*, vol. 18, no. 20, Art. no. 20, Jan. 2021, doi: 10.3390/ijerph182010900.
- [11] "Potential health effects of PFAS chemicals | ATSDR." Accessed: Jul. 03, 2024. [Online]. Available: <https://www.atsdr.cdc.gov/pfas/health-effects/index.html>
- [12] "Final Recommended Aquatic Life Criteria and Benchmarks for Select PFAS; Correction," Federal Register. Accessed: Apr. 21, 2025. [Online]. Available: <https://www.federalregister.gov/documents/2024/11/13/2024-26228/final-recommended-aquatic-life-criteria-and-benchmarks-for-select-pfas-correction>
- [13] A. Salemi and T. C. Schmidt, "Recent Advances and Applications of Passive Sampling Devices," vol. 41, pp. 22–24, Nov. 2023.
- [14] J. M. Thompson, C.-H. Hsieh, and R. G. Luthy, "Modeling Uptake of Hydrophobic Organic Contaminants into Polyethylene Passive Samplers," *Environ. Sci. Technol.*, vol. 49, no. 4, pp. 2270–2277, Feb. 2015, doi: 10.1021/es504442s.
- [15] Y. Fang *et al.*, "Removal of Per- and Polyfluoroalkyl Substances (PFASs) in Aqueous Film-Forming Foam (AFFF) Using Ion-Exchange and Nonionic Resins," *Environ. Sci. Technol.*, vol. 55, no. 8, pp. 5001–5011, Apr. 2021, doi: 10.1021/acs.est.1c00769.

- [16] Y. He, X. Cheng, S. J. Gunjal, and C. Zhang, “Advancing PFAS Sorbent Design: Mechanisms, Challenges, and Perspectives,” *ACS Mater. Au*, vol. 4, no. 2, pp. 108–114, Mar. 2024, doi: 10.1021/acsmaterialsau.3c00066.
- [17] “Passive sampler designed for per- and polyfluoroalkyl substances using polymer-modified organosilica adsorbent - Hartmann - 2021 - AWWA Water Science - Wiley Online Library.” Accessed: Mar. 10, 2025. [Online]. Available: https://awwa.onlinelibrary.wiley.com/doi/full/10.1002/aws2.1237?utm_source=chatgpt.com
- [18] C. Gardiner *et al.*, “Field Validation of a Novel Passive Sampler for Dissolved PFAS in Surface Waters,” *Environmental Toxicology and Chemistry*, vol. 41, no. 10, pp. 2375–2385, 2022, doi: 10.1002/etc.5431.
- [19] “Passive sampling as a tool for obtaining reliable analytical information in environmental quality monitoring | Analytical and Bioanalytical Chemistry.” Accessed: Mar. 10, 2025. [Online]. Available: <https://link.springer.com/article/10.1007/s00216-009-3244-4>
- [20] P. Mayer, J. Tolls, J. L. M. Hermens, and D. Mackay, “Peer Reviewed: Equilibrium Sampling Devices,” *Environ. Sci. Technol.*, vol. 37, no. 9, pp. 184A–191A, May 2003, doi: 10.1021/es032433i.
- [21] F. Y. Lai, C. Rauert, L. Gobelius, and L. Ahrens, “A critical review on passive sampling in air and water for per- and polyfluoroalkyl substances (PFASs),” *TrAC Trends in Analytical Chemistry*, vol. 121, p. 115311, Dec. 2019, doi: 10.1016/j.trac.2018.11.009.
- [22] B. Vrana *et al.*, “Passive sampling techniques for monitoring pollutants in water,” *TrAC Trends in Analytical Chemistry*, vol. 24, no. 10, pp. 845–868, Nov. 2005, doi: 10.1016/j.trac.2005.06.006.
- [23] Y. Jeong, A. Schäffer, and K. Smith, “A comparison of equilibrium and kinetic passive sampling for the monitoring of aquatic organic contaminants in German rivers,” *Water Res.*, vol. 145, pp. 248–258, Nov. 2018, doi: 10.1016/j.watres.2018.08.016.
- [24] B. Medon *et al.*, “A field-validated equilibrium passive sampler for the monitoring of per- and polyfluoroalkyl substances (PFAS) in sediment pore water and surface water,” *Environmental Science: Processes & Impacts*, vol. 25, no. 5, pp. 980–995, 2023, doi: 10.1039/D2EM00483F.
- [25] A. S. Joyce and R. M. Burgess, “Using performance reference compounds to compare mass transfer calibration methodologies in passive samplers deployed in the water column,” *Environmental Toxicology and Chemistry*, vol. 37, no. 8, pp. 2089–2097, Aug. 2018, doi: 10.1002/etc.4167.
- [26] M. E. Bartkow, K. C. Jones, K. E. Kennedy, N. Holling, D. W. Hawker, and J. F. Müller, “Evaluation of performance reference compounds in polyethylene-based passive air samplers,” *Environmental Pollution*, vol. 144, no. 2, pp. 365–370, Nov. 2006, doi: 10.1016/j.envpol.2005.12.043.
- [27] H.-H. Liu, C. S. Wong, and E. Y. Zeng, “Recognizing the Limitations of Performance Reference Compound (PRC)-Calibration Technique in Passive Water Sampling,” *Environ. Sci. Technol.*, vol. 47, no. 18, pp. 10104–10105, Sep. 2013, doi: 10.1021/es403353d.
- [28] S. E. Hale, B. Canivet, T. Rundberget, H. A. Langberg, and I. J. Allan, “Using Passive Samplers to Track per and Polyfluoroalkyl Substances (PFAS) Emissions From the Paper Industry: Laboratory Calibration and Field Verification,” *Front. Environ. Sci.*, vol. 9, Dec. 2021, doi: 10.3389/fenvs.2021.796026.
- [29] V. Fauvelle *et al.*, “Dealing with Flow Effects on the Uptake of Polar Compounds by Passive Samplers,” *Environ. Sci. Technol.*, vol. 51, no. 5, pp. 2536–2537, Mar. 2017, doi: 10.1021/acs.est.7b00558.

- [30] L. Wang, R. Liu, X. Liu, and H. Gao, "Sampling Rate of Polar Organic Chemical Integrative Sampler (POCIS): Influence Factors and Calibration Methods," *Applied Sciences*, vol. 10, no. 16, Art. no. 16, Jan. 2020, doi: 10.3390/app10165548.
- [31] C. Harman, I. J. Allan, and P. S. B  uerlein, "The Challenge of Exposure Correction for Polar Passive Samplers—The PRC and the POCIS," *Environ. Sci. Technol.*, vol. 45, no. 21, pp. 9120–9121, Nov. 2011, doi: 10.1021/es2033789.
- [32] N. Mazzella, S. Lissalde, S. Moreira, F. Delmas, P. Mazellier, and J. N. Huckins, "Evaluation of the Use of Performance Reference Compounds in an Oasis-HLB Adsorbent Based Passive Sampler for Improving Water Concentration Estimates of Polar Herbicides in Freshwater," *Environ. Sci. Technol.*, vol. 44, no. 5, pp. 1713–1719, Mar. 2010, doi: 10.1021/es902256m.
- [33] C. Harman, I. J. Allan, and E. L. M. Vermeirssen, "Calibration and use of the polar organic chemical integrative sampler—a critical review," *Environmental Toxicology and Chemistry*, vol. 31, no. 12, pp. 2724–2738, Dec. 2012, doi: 10.1002/etc.2011.
- [34] R. Z. Hahn, C. Augusto do Nascimento, and R. Linden, "Evaluation of Illicit Drug Consumption by Wastewater Analysis Using Polar Organic Chemical Integrative Sampler as a Monitoring Tool," *Front. Chem.*, vol. 9, Mar. 2021, doi: 10.3389/fchem.2021.596875.
- [35] Y. Qi, H. Cao, W. Pan, C. Wang, and Y. Liang, "The role of dissolved organic matter during Per- and Polyfluorinated Substance (PFAS) adsorption, degradation, and plant uptake: A review," *Journal of Hazardous Materials*, vol. 436, p. 129139, Aug. 2022, doi: 10.1016/j.jhazmat.2022.129139.
- [36] S. Yu and Y. Zhou, "[Influence of Natural Dissolved Organic Matter on the Passive Sampling Technique and its Application]," *Huan Jing Ke Xue*, vol. 36, no. 8, pp. 2895–2899, Aug. 2015.
- [37] K. Booij *et al.*, "Passive Sampling in Regulatory Chemical Monitoring of Nonpolar Organic Compounds in the Aquatic Environment," *Environ. Sci. Technol.*, vol. 50, no. 1, pp. 3–17, Jan. 2016, doi: 10.1021/acs.est.5b04050.
- [38] C. Gerena, "The Evolving Economic Role of Baltimore's Waterfront and Location," 2003.
- [39] "Chesapeake Bay Journal: History of dredging reveals deeper need to understand Bay's bottom line - July/August 2000." Accessed: Apr. 21, 2025. [Online]. Available: <https://web.archive.org/web/20070928160802/https://www.bayjournal.com/article.cfm?article=1322>
- [40] "History of Baltimore_1.pdf." Accessed: Mar. 10, 2025. [Online]. Available: https://planning.baltimorecity.gov/sites/default/files/History%20of%20Baltimore_1.pdf
- [41] M. A. Aubourg *et al.*, "Use of electron microscopy to determine presence of coal dust in a neighborhood bordering an open-air coal terminal in Curtis Bay, Baltimore, Maryland, USA," *Science of The Total Environment*, vol. 957, p. 176842, Dec. 2024, doi: 10.1016/j.scitotenv.2024.176842.
- [42] R. Kobell and V. Smith, "Protecting Baltimore's Water Supply from 'Forever Chemicals,'" 2021.
- [43] "Water Issues – Blue Water Baltimore." Accessed: Mar. 10, 2025. [Online]. Available: <https://bluewaterbaltimore.org/baltimore-city-water-issues/>
- [44] P. R. Network, "PFAS Investigation Program," Potomac Riverkeeper Network. Accessed: Mar. 10, 2025. [Online]. Available: <https://www.potomacriverkeepernetwork.org/pfas-investigation-program/>
- [45] "'Forever chemicals' contamination at Defense Department sites threatens Chesapeake Bay fish | Environmental Working Group." Accessed: Mar. 10, 2025. [Online]. Available: <https://www.ewg.org/news-insights/news/2021/08/forever-chemicals->

- contamination-defense-department-sites-threatens
- [46] “Maryland and PFAS,” Department of the Environment. Accessed: Mar. 10, 2025. [Online]. Available: <https://mde.maryland.gov/PublicHealth/Pages/default.aspx>
 - [47] “Improving Understanding and Coordination of Science Activities for Per- and Polyfluoroalkyl Substances (PFAS) in the Chesapeake Bay Watershed,” STAC. Accessed: Mar. 13, 2025. [Online]. Available: <https://www.chesapeake.org/stac/document-library/improving-understanding-and-coordination-of-science-activities-for-per-and-polyfluoroalkyl-substances-pfas-in-the-chesapeake-bay-watershed/>
 - [48] “PRKN Mapping of MDE PFAS Monitoring Data for Fish Consumption.” Accessed: Jul. 10, 2024. [Online]. Available: <https://potomacriverkeep.maps.arcgis.com/apps/mapviewer/index.html?webmap=9821bc24ab434ded8592216d19fb86be>
 - [49] K. He *et al.*, “Retention of per- and polyfluoroalkyl substances by syringe filters,” *Environ Chem Lett*, vol. 22, no. 4, pp. 1569–1579, Aug. 2024, doi: 10.1007/s10311-024-01718-2.
 - [50] M. Vakili *et al.*, “Regeneration of exhausted adsorbents after PFAS adsorption: A critical review,” *Journal of Hazardous Materials*, vol. 471, p. 134429, Jun. 2024, doi: 10.1016/j.jhazmat.2024.134429.
 - [51] L. Blaney and K. He, “Ion Exchange Membranes and Fibers as Passive Samplers for Chemically-diverse PFAS Final Report (ER20-1073).” Dec. 2021. Accessed: Mar. 10, 2025. [Online]. Available: <https://sepub-prod-0001-124733793621-us-gov-west-1.s3.us-gov-west-1.amazonaws.com/s3fs-public/2024-02/ER20-1073%20Final%20Report.pdf?VersionId=4orwQT3VaSWnbkdtjhEwQZlaxUemiLCb>
 - [52] Y. Wang, S. B. Darling, and J. Chen, “Selectivity of Per- and Polyfluoroalkyl Substance Sensors and Sorbents in Water,” *ACS Appl. Mater. Interfaces*, vol. 13, no. 51, pp. 60789–60814, Dec. 2021, doi: 10.1021/acsami.1c16517.
 - [53] T. M. H. Nguyen *et al.*, “Influences of Chemical Properties, Soil Properties, and Solution pH on Soil–Water Partitioning Coefficients of Per- and Polyfluoroalkyl Substances (PFASs),” *Environ. Sci. Technol.*, vol. 54, no. 24, pp. 15883–15892, Dec. 2020, doi: 10.1021/acs.est.0c05705.
 - [54] “PFAS — Per- and Polyfluoroalkyl Substances.” Accessed: Jul. 02, 2024. [Online]. Available: https://pfas-1.itrcweb.org/#1_3
 - [55] “Is the Chesapeake Bay fresh or salty?,” Chesapeake Bay. Accessed: Jul. 03, 2024. [Online]. Available: <https://www.chesapeakebay.net/news/blog/fresh-or-salty-bays-salinity-makes-a-big-difference-to-underwater-life>
 - [56] “Physical Characteristics,” Chesapeake Bay Program. Accessed: Mar. 11, 2025. [Online]. Available: <https://www.chesapeakebay.net/discover/ecosystem/physical-characteristics>
 - [57] “Eyes on the Bay: Your home for Maryland tidal water quality data, downloads and visualizations,” Eyes on the Bay. Accessed: Mar. 11, 2025. [Online]. Available: [//eyesonthebay.dnr.maryland.gov/eyesonthebay/index.cfm](http://eyesonthebay.dnr.maryland.gov/eyesonthebay/index.cfm)
 - [58] R. P. Schwarzenbach, P. M. Gschwend, and D. M. Imboden, “Environmental Organic Chemistry (3rd Edition),” in *Environmental Organic Chemistry (3rd Edition)*, Third Edition., Wiley, 2017, pp. 275–280.
 - [59] H.-X. Zhou, “Interactions of Macromolecules with Salt Ions: An Electrostatic Theory for the Hofmeister Effect,” *Wiley*, Jul. 2005, doi: 10.1002/prot.20500.
 - [60] H. E. Hartnett, “Dissolved Organic Matter (DOM),” in *Encyclopedia of Geochemistry: A Comprehensive Reference Source on the Chemistry of the Earth*, W. M. White, Ed., Cham: Springer International Publishing, 2018, pp. 375–378. doi: 10.1007/978-3-319-

- 39312-4_155.
- [61] N. Senesi, T. M. Miano, M. R. Provenzano, and G. Brunetti, "Spectroscopic and compositional comparative characterization of I.H.S.S. reference and standard fulvic and humic acids of various origin," *Science of The Total Environment*, vol. 81–82, pp. 143–156, Jun. 1989, doi: 10.1016/0048-9697(89)90120-4.
 - [62] Q.-L. Fu *et al.*, "Development of a Nontargeted Algorithm for Per- and Polyfluoroalkyl Substances in the FT-ICR Mass Spectra of Complex Organic Mixtures," *Anal. Chem.*, Mar. 2025, doi: 10.1021/acs.analchem.4c06674.
 - [63] Q. Lai *et al.*, "Effects of Dissolved Organic Matter (DOM) on Perfluorooctanoic Acid (PFOA) in a Seagoing River—A Case Study of the Wanggang River Flowing into the East China Sea," *Water*, vol. 14, no. 21, Art. no. 21, Jan. 2022, doi: 10.3390/w14213580.
 - [64] W. Wen *et al.*, "Bioconcentration of perfluoroalkyl substances by *Chironomus plumosus* larvae in water with different types of dissolved organic matters," *Environmental Pollution*, vol. 213, pp. 299–307, Jun. 2016, doi: 10.1016/j.envpol.2016.02.018.
 - [65] Y. Li *et al.*, "Determining obstructive or promoting effects of anions and DOM on phosphate transport combining with Donnan dialysis and selective electrodialysis," *Desalination*, vol. 586, p. 117786, Oct. 2024, doi: 10.1016/j.desal.2024.117786.
 - [66] P. Wang, J. K. Challis, Z.-X. He, C. S. Wong, and E. Y. Zeng, "Effects of biofouling on the uptake of perfluorinated alkyl acids by organic-diffusive gradients in thin films passive samplers," *Environ. Sci.: Processes Impacts*, vol. 24, no. 2, pp. 242–251, Feb. 2022, doi: 10.1039/D1EM00436K.
 - [67] X. C. Hu *et al.*, "Detection of Poly- and Perfluoroalkyl Substances (PFASs) in U.S. Drinking Water Linked to Industrial Sites, Military Fire Training Areas, and Wastewater Treatment Plants," *Environ. Sci. Technol. Lett.*, vol. 3, no. 10, pp. 344–350, Oct. 2016, doi: 10.1021/acs.estlett.6b00260.
 - [68] "Healthy Harbor Initiative," Waterfront Partnership of Baltimore. Accessed: Mar. 13, 2025. [Online]. Available: <https://www.waterfrontpartnership.org/healthy-harbor-initiative>
 - [69] L. P. Arendsen, R. Thakar, and A. H. Sultan, "The Use of Copper as an Antimicrobial Agent in Health Care, Including Obstetrics and Gynecology," *Clin Microbiol Rev*, vol. 32, no. 4, pp. e00125-18, Aug. 2019, doi: 10.1128/CMR.00125-18.
 - [70] G. Grass, C. Rensing, and M. Solioz, "Metallic Copper as an Antimicrobial Surface," *Appl Environ Microbiol*, vol. 77, no. 5, pp. 1541–1547, Mar. 2011, doi: 10.1128/AEM.02766-10.
 - [71] M. M. Schultz, C. P. Higgins, C. A. Huset, R. G. Luthy, D. F. Barofsky, and J. A. Field, "Fluorochemical Mass Flows in a Municipal Wastewater Treatment Facility," *Environ. Sci. Technol.*, vol. 40, no. 23, pp. 7350–7357, Dec. 2006, doi: 10.1021/es061025m.
 - [72] M. S. Ahmed *et al.*, "Corrosion of Copper in a Tropical Marine Atmosphere Rich in H₂S Resulting from the Decomposition of Sargassum Algae," *Metals*, vol. 13, no. 5, Art. no. 5, May 2023, doi: 10.3390/met13050982.
 - [73] W. Cai *et al.*, "Effect of heavy metal *co*-contaminants on the sorption of thirteen anionic *per*- and *poly*-fluoroalkyl substances (PFAS) in soils," *Science of The Total Environment*, vol. 905, p. 167188, Dec. 2023, doi: 10.1016/j.scitotenv.2023.167188.
 - [74] A. Chaudhary, M. Usman, W. Cheng, S. Haderlein, J.-F. Boily, and K. Hanna, "Heavy-Metal Ions Control on PFAS Adsorption on Goethite in Aquatic Systems," *Environ Sci Technol*, vol. 58, no. 45, pp. 20235–20244, Nov. 2024, doi: 10.1021/acs.est.4c10068.
 - [75] J. Kim, X. Xin, G. L. Hawkins, Q. Huang, and C.-H. Huang, "Occurrence, Fate, and Removal of Per- and Polyfluoroalkyl Substances (PFAS) in Small- and Large-Scale Municipal Wastewater Treatment Facilities in the United States," *ACS EST Water*, vol.

- 4, no. 12, pp. 5428–5436, Dec. 2024, doi: 10.1021/acsestwater.4c00541.
- [76] J. A. Batista-Andrade, E. Diaz, D. Iglesias Vega, E. Hain, M. R. Rose, and L. Blaney, “Spatiotemporal analysis of fluorescent dissolved organic matter to identify the impacts of failing sewer infrastructure in urban streams,” *Water Research*, vol. 229, p. 119521, Feb. 2023, doi: 10.1016/j.watres.2022.119521.
 - [77] J. A. Batista-Andrade, D. Iglesias Vega, A. McClain, and L. Blaney, “Using multilinear regressions developed from excitation-emission matrices to estimate the wastewater content in urban streams impacted by sanitary sewer leaks and overflows,” *Science of The Total Environment*, vol. 906, p. 167736, Jan. 2024, doi: 10.1016/j.scitotenv.2023.167736.
 - [78] J. A. Batista-Andrade, C. Welty, D. Iglesias Vega, A. McClain, and L. Blaney, “Geospatial Variability of Fluorescent Dissolved Organic Matter in Urban Watersheds: Relationships with Land Cover and Wastewater Infrastructure,” *Environ. Sci. Technol.*, vol. 58, no. 17, pp. 7529–7542, Apr. 2024, doi: 10.1021/acs.est.3c07925.
 - [79] S. Björklund, E. Weidemann, and S. Jansson, “Emission of Per- and Polyfluoroalkyl Substances from a Waste-to-Energy Plant—Occurrence in Ashes, Treated Process Water, and First Observation in Flue Gas,” *Environ Sci Technol*, vol. 57, no. 27, pp. 10089–10095, Jun. 2023, doi: 10.1021/acs.est.2c08960.

ProQuest Number: 31998097

INFORMATION TO ALL USERS

The quality and completeness of this reproduction is dependent on the quality and completeness of the copy made available to ProQuest.



Distributed by
ProQuest LLC a part of Clarivate (2025).
Copyright of the Dissertation is held by the Author unless otherwise noted.

This work is protected against unauthorized copying under Title 17,
United States Code and other applicable copyright laws.

This work may be used in accordance with the terms of the Creative Commons license or other rights statement, as indicated in the copyright statement or in the metadata associated with this work. Unless otherwise specified in the copyright statement or the metadata, all rights are reserved by the copyright holder.

ProQuest LLC
789 East Eisenhower Parkway
Ann Arbor, MI 48108 USA